Open access • Journal Article • DOI:10.1051/RPHYSAP:01980001503047700

Short term thermal energy storage — Source link

A. Abhat

Institutions: University of Stuttgart

Published on: 01 Mar 1980

Topics: Thermal energy storage, Storage water heater, Waste heat, Latent heat and Renewable heat

Short term thermal energy storage

A. Abhat

Revue Phys. Appl. **15** (1980) 477-501 MARS 1980, PAGE 477

Classification
Physics Abstracts
44.00

Short term thermal energy storage

A. Abhat

Institut für Kernenergetik und Energiesysteme, University of Stuttgart, Stuttgart, FRG

(*Reçu le 20 septembre 1979, accepté le 9 novembre 1979*)

Résumé. — Cet article passe en revue le problème du stockage d'énergie thermique à court terme pour les applications du chauffage solaire à basse température. Les techniques d'accumulation avec ou sans changement de phase sont discutées en insistant tout particulièrement sur la première. Les exigences concernant les systèmes à stockage d'eau chaude sont données et l'importance du phénomène de stratification dans les réservoirs est mise en relief. En ce qui concerne le stockage par chaleur latente, nous considérons en détail à la fois les aspects *matériaux* et *échangeurs*. L'exemple d'un réservoir passif à chaleur latente employant un échangeur tubulaire à ailettes illustre les problèmes de transfert de chaleur dans les matériaux utilisés, en général faiblement conducteurs de la chaleur. Un certain nombre de données économiques concernant le stockage de chaleur sont aussi présentées.

Abstract. — The present paper reviews the problem of short term thermal energy storage for low temperature solar heating applications. The techniques of sensible and latent heat storage are discussed, with particular emphasis on the latter. Requirements for hot water storage subsystems are provided and the importance of stratification in hot water storage tanks is described. Concerning latent heat storage, both material and heat exchanger aspects are considered in detail. The example of a passively operating latent heat store employing a finned heat pipe heat exchanger is used to elaborate upon the heat transfer problems in the generally poorly conducting phase change heat storage materials. Finally, some data pertaining to the current economics of heat storage are presented.

1. **Introduction.** — 1.1 THE NECESSITY OF THERMAL STORAGE IN SOLAR HEATING APPLICATIONS. — Solar energy is an intermittent energy source. The availability of solar energy is affected by the daily day-night cycle and by the seasons, as well as by the changes in weather that may be caused by the appearance of clouds, rain or snow. The use of solar energy as an effective energy source for heating purposes is further complicated by the fact that the energy demand for most heating applications is out of phase with the availability of solar energy. In residential applications, for example, as seen in figure 1, the bulk of the annual heating load occurs during the winter months and the greater part of the daily heating load exists in the evenings. At both these times, the supply of solar energy is, on the other hand, the minimum.

The viability of solar energy as an energy source can hence be established only by including a thermal store within the solar heating system. Thermal stores of small heat storage capacity can help neutralize the fluctuations on the load side introduced by minor interruptions in weather, e.g. by the appearance of clouds. Larger thermal stores, on the other hand, can store enough heat while the sun is shining to meet the energy demands for a 24-hour (i.e. day-night) period or a 12-month (i.e. summer-winter) period. The former type of storage is called *daily or short-term storage* while the latter is termed *annual, seasonal or long-term storage*. Short-term storage is a dynamic system that undergoes a daily charge/discharge cycle and hence participates actively in the function of the solar heating system. The optimum size of the storage itself depends on the application concerned and is a complicated function of several factors, such as weather data, building heat load and heat losses, collector area and efficiency, storage temperature, storage heat losses, solar fraction of the total heat load, costs of the storage medium, container, heat exchanger and pumps, cost of auxiliary energy, etc. It is, however, out of the scope of this paper to determine the optimum size, which is generally computed with the aid of computer simulation programs that take these factors in consideration.

The present paper shall deal with the discussion of short-term storage at low temperatures. We shall consider here storage systems for solar space heating and domestic hot water production, systems in which the application temperature generally varies between 20 to 80 °C. Storage temperatures between 20 °C and 80 °C shall hence be considered.

1.2 DESIRED CHARACTERISTICS OF A THERMAL STORE. — Irrespective of their size, all thermal stores incorporated within a solar heating system must possess

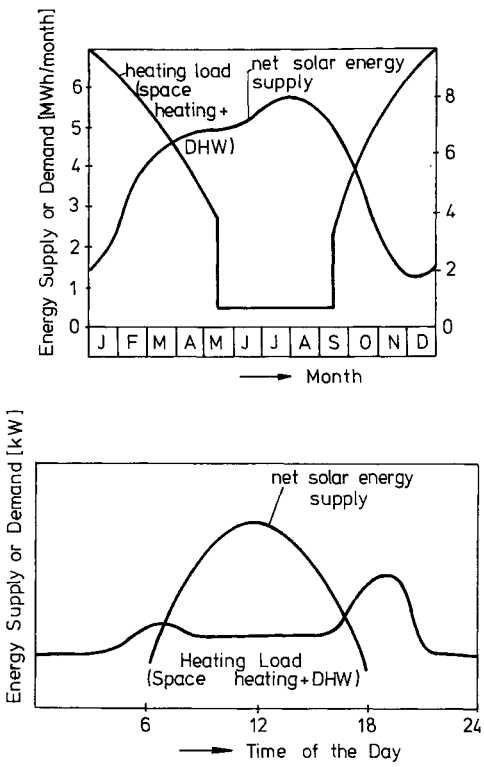

Fig. 1. — Temporal variation of daily and annual supply of solar energy and of energy demand.

certain properties. The desired characteristics of a thermal store are listed in table I.

The choice of suitable techniques for thermal energy storage must be based on all these criteria and appropriate trade-off must be made in their selection.

Table I. — *Desired characteristics of a thermal store.*

- Compact ; large storage capacity per unit mass and volume.
- High storage efficiency.
- Heat storage medium with suitable properties in the operating temperature range.
- Uniform temperature.
- Capability to charge and discharge with the largest heat input/output rates but without large temperature gradients.
- Ability to undergo large number of charging/discharging cycles without loss in performance and storage capacity.
- Small self-discharging rate i.e. negligible heat losses to the surroundings.
- Long life.
- Inexpensive.

1.3 TECHNIQUES FOR THERMAL ENERGY STORAGE. — An overview of the major techniques for thermal energy storage for solar heating applications is presented in figure 2.

At low temperatures, solar heat is essentially stored in two ways :

1) *Sensible heat storage* : as sensible heat in solids, e.g. rocks, or liquids, e.g. water. The heat storage

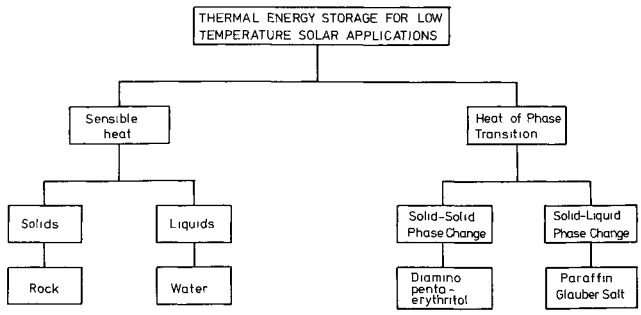

Fig. 2. — Major techniques for thermal energy storage at low temperatures.

medium thereby experiences an increase in temperature without undergoing a change in its phase.

2) *Latent heat storage* : as latent heat of fusion in suitable chemical compounds, e.g. paraffin waxes and inorganic salts. The heat storage medium absorbs the heat added and undergoes a phase transition from the solid to the liquid state at a desired temperature within the operating temperature range. For pure substances, the heat storage takes place at a constant temperature that corresponds to the melting point of the substance.

In certain chemicals, e.g. Diaminopentaerythritol, heat may also be stored as the heat of crystallization, as the substance is transformed from one solid phase to another solid phase. The stored heat is recovered in a likewise manner as the original solid phase is obtained back.

In addition to these two methods, heat storage in the form of heat of reaction is also finding increasing interest lately. This shall, however, not be the subject of discussion in the present paper.

Thermal stores wherein energy is stored as sensible heat in rocks or water are today off-the-shelf items and are readily available as components of solar heating systems. Latent heat storage, on the other hand, is a developing technology which has found considerable interest in recent times due to its operational advantages of smaller temperature swings, lower required solar collector temperature, and smaller size and lower weight per unit of storage capacity.

Major comparison criteria for different types of heat storage media for sensible and latent heat storage and for the heat transfer properties and life of different types of thermal stores are presented in table II. No method of thermal energy storage is, however, at the moment, perfect and trade-offs must be made in selecting a particular type of thermal store.

In the present report, we shall briefly discuss the method of sensible heat storage in water with special emphasis on stratification in storage water tanks. On the other hand, the method of latent heat storage — henceforth abbreviated LTES — shall be discussed

Table II. — *Comparison of different storage techniques for solar space heating and hot water production applications.*

	Sensible heat storage		Latent heat storage phase change material (solid-liquid)
	Water	Rock	
A) *Comparison between different heat storage media*			
a) Operating temperature range	limited 0-100 °C	large	large, depending on the choice of the material
b) Specific heat	high	low	medium
c) Thermal conductivity	low, convection effects improve the heat transfer rate	low	very low ; insulating properties
d) Thermal storage capacity per unit mass and unit volume for small temperature differences	low	low	high (*)
e) Stability to thermal cycling	good	good	insufficient data
f) Availability	overall	almost overall	dependent on the choice of material
g) Cost	cheap	cheap	expensive
B) *Comparison of heat transfer properties and life of different types of thermal stores*			
a) Required heat exchanger geometry	simple	simple	complex
b) Temperature gradients during charging and discharging	large	large	small
c) Thermal stratification effect	existent, works positively	existent, works positively	generally non-existent with proper choice of material
d) Simultaneous charging and discharging	possible	not possible	possible with appropriate selection of heat exchanger
e) Integration with solar heating/cooling systems	direct integration with water systems	direct integration with air systems	indirect integration
f) Costs for pumps, fans, etc.	low	high	low
g) Corrosion with conventional materials of construction	corrosion eliminated through corrosion inhibitors	non-corrosive	presently only limited information available
h) Life	long	long	presently only limited information available

(*) Through use of latent heat of fusion.

in greater detail. While most of the discussion that follows holds for LTES systems in general, special attention shall be given to thermal stores operating in the temperature range 20-80 °C.

2. **Fundamental considerations of sensible and latent heat storage.** — 2.1 PHYSICAL PRINCIPLES. — When energy in the form of heat is added to a substance, an increase in its internal energy results. The well-known consequence of this is either an increase in temperature (sensible heating) or a change of phase (latent heating). Both these effects are depicted by the temperature-time diagram of figure 3 drawn for constant heat addition into a pure crystalline substance.

Starting with an initial solid state at point O, heat addition to the substance first causes sensible heating of the solid (region O-A) followed by a solid-to-liquid phase change (region A-B), sensible heating of the liquid (region B-C), liquid-to-vapor phase change (region C-D) and sensible heating of the vapor (region D-E). During each of these processes, heat is absorbed or stored within the substance, the magnitude of which is given by the relationships,

$$Q = MCp_i(T_e - T_b) \quad \text{for sensible heating} \qquad (1)$$

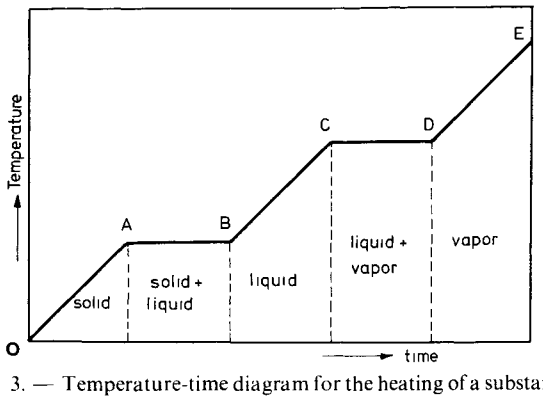

Fig. 3. — Temperature-time diagram for the heating of a substance.

and

$$Q = ML_{i-j} \qquad \text{for latent heating} \qquad (2)$$

where

M is the mass of the substance,

Cp_i is the specific heat of the phase « i » of the substance, where « i » represents the solid (S), liquid (L), or vapor (V) phases,

T_e and T_b are the temperatures of the substance at the beginning and end of a time interval during which sensible heating occurs,

and

L_{i-j} is the latent heat required to change the substance from an existing phase « i » to a new phase « j », where « i » and « j » represent the solid, liquid or vapor phases.

To understand the physical arguments behind the temperature-time diagram of figure 3, we refer to the molecular theory of matter [8]. Every substance comprises of a large number of molecules that are in constant interaction with each other. The interaction between the molecules can be well represented by supposing that they are surrounded by a conservative field of force, not necessarily symmetrical in character, and that the resultant force on any given molecule is the vector sum of the forces exerted on it separately by the other molecules. At all distances greater than what may loosely be described as a « molecular diameter » the force between two neighbouring molecules is attractive as a consequence of the mutual polarization of the charges of which the different molecules are compounded. At short distances, less than one molecular diameter, the intense electrostatic repulsion between the electrons in the outer shells of two neighbouring molecules renders the interaction between the molecules repulsive. A soft medium-range attractive field and a hard short-range repulsive field thus characterizes the interaction between all molecules. Upto a certain atomic distance Δ_0, the net force on a molecule is hence repulsive and beyond Δ_0, it is attractive. At this distance Δ_0, the mutual potential energy of the molecules is at a minimum.

Another important feature of the microscope picture of matter is the thermal motion of the molecules. It is now well recognized that the temperature of any substance is a measure of the mean kinetic energy of the molecules. Thus only at absolute zero, the molecules may be imagined to be at rest and as the temperature of the substance is raised, the velocities of the molecules increase. Even though the substance may appear to be at rest, the molecules comprising it are in a state of rapid motion, particularly in fluids — an effect now well known as the Brownian movement of molecules.

Now referring back to figure 3, the substance is initially in a solid crystalline state with some temperature T_0 at the point O. This state is characterized by a state of high order and a low entropy in the configuration of the molecules comprising the substance. The molecules remain for long periods of time in the vicinity of fixed lattice sites, whose positions are marked by a minimum in the mean potential energy of each molecule. However, as the temperature of the solid is above absolute zero the molecules are not at rest, but perform continuous small oscillations about their lattice positions under the influence of the forces exerted by the other molecules. The oscillation of each molecule is then a superposition of very larger number of harmonic motions, with frequencies depending on the intermolecular forces. As heat is added to the substance, the amplitude of the oscillations, and thereby the mean kinetic energy of the molecules, is increased. This increase in mean kinetic energy is measured as an increase in temperature of the substance, as seen in the sensible heating region O-A in figure 3.

As the amplitude of oscillations increase, a point is eventually reached — just below the melting point of the substance — when the individual molecules are able to leave their lattice sites and move either into interstitial positions with a displacement of the surrounding molecules, or to sites vacated by other molecules. It is possible for this to happen fairly extensively without the destruction of the lattice arrangement as a whole. However, at the melting point — point A in figure 3 — the agitation becomes sufficiently great for the majority of the molecules to leave their lattice sites permanently and the lattice disintegrates.

The process of melting is hence regarded as the transition of a substance from a state of order to one of disorder among the molecules. As long as melting of a substance is taking place, the energy added to the substance in the form of heat is spent up in the movement and collision of the molecules and causes an increase in the potential energy of the molecules. Consequently, an increase in the mean kinetic energy of the molecules, and hence of the temperature of the solid-liquid mixture, does not take place. This effect is exhibited by the line A-B in figure 3, which represents the change of phase of the substance from the solid to the liquid state. Furthermore, in comparison with the solid state, the mass density of the liquid, defined as the product of the molecular mass and the number of molecules per

unit volume, is smaller as the element of volume occupied by each individual molecule is now larger. An increase in the volume occupied by the substance in its liquid state hence occurs.

In the liquid phase — region B-C in figure 3 — the mean kinetic energy of the molecules once again increases, so that an increase in temperature results. Associated with the temperature increase is a decrease in mass density or an increase in volume due to the more frequent and stronger molecular collisions.

Further heat addition brings us to the boiling point of the substance — point C in figure 3. The energy added overcomes any existing forces of molecular attraction and allows the escape of the more energetic of the molecules at the free surface of the liquid, which now enter the vapor phase of the substance. The vapor phase is characterized by a state of yet higher disorder and, as in the case of solid-liquid phase change, the energy added is used to increase the potential energy of the molecules. Along the line C-D, no increase in temperature of the substance hence takes place. The increase in volume is, however, now substantially large.

Beyond the point D, the vapor molecules behave similar to the liquid molecules in region B-C. Any heat added causes an increase in the mean kinetic energy of the molecules and thereby an increase in the vapor temperature. The molecules are now in a state of constant and rapid motion and the intermolecular collisions are very frequent. The volume increase associated with temperature rise of the vapor is hence quite large.

The amount of heat added to a substance in the various sensible heating and latent heating regions has been given earlier by equations (1) and (2). Using these equations the total amount of heat added between the points O and E may be written as,

$$Q = M\left[\int_{T_0}^{T_A} Cp_S(T)\,dT + \Delta H_F + \int_{T_B}^{T_C} Cp_L(T)\,dT + \right.$$
$$\left. + \Delta H_V + \int_{T_D}^{T_E} Cp_V(T)\,dT\right] \quad (3)$$

where

M is the mass of the substance,

Cp_S, Cp_L and Cp_V are respectively the specific heats of the solid, liquid and vapor phases of the substance and are a function of temperature,

ΔH_F is the enthalpy or latent heat of fusion and equals L_{S-L}

and

ΔH_V is the enthalpy or latent heat of vaporization and equals L_{L-V}.

For a pure substance, the amount of heat stored Q described by equation (3) above may be recovered as the substance is cooled from a vapor phase at temperature T_E to a solid phase at temperature T_0. The mechanisms of sensible cooling of the vapor, liquid and solid, as well as the processes of condensation and freezing could then be explained in a likewise manner using the molecular theory of matter.

Latent heat thermal energy storage systems operate in the region AB of figure 3, i.e. the heat storage substance undergoes a phase change from the solid to the liquid state at constant temperature during heat addition and recovers its original solid phase during heat removal. The process of heat addition results in charging of the storage, while heat removal causes discharging of the storage. The solid-liquid phase change region is selected for LTES systems against the liquid-vapor phase change region inspite of the far larger latent heat storage capacity per unit mass of the latter, essentially because the volume change during the solid-liquid phase change is relatively small. An added advantage with solid-liquid phase change is that it takes place at constant pressure, thus eliminating the need for pressure vessels as containment.

2.2 THE THEORY OF CRYSTALLIZATION. — Crystallization commences with the formation of solid nuclei, which consume the liquid around them as they grow. The formation of solid nuclei and their growth are hence necessary factors for obtaining the new solid phase from a liquid (melt). Starting with a homogeneous concentration of the liquid phase, freezing can result in non-homogeneous distribution in the solid state. Information pertaining to any change in concentration or degree of segregation that may exist in the solid phase is hence required and this can be gained from the Phase or Equilibrium Diagrams.

2.2.1 *Phase diagrams.* — A phase diagram is basically a summary of the various equilibria observable between the components involved in a multi-component system as function of the relevant variables, e.g. composition, temperature and pressure. Phase diagrams can be classified in different categories depending on whether the components are soluble in the solid phase or whether compounds are formed during freezing. Some of the important systems described by phase diagrams are [21] :

A) complete solubility of the components in the solid and liquid phases,

B) simple eutectic system with no solubility in the solid phase,

C) eutectic system with limited solubility in the solid phase,

D) pertitectic system,

E) formation of compounds with complete solid solution, and with no solid solution but congruent and incongruent melting compounds.

Phase diagrams for binary systems of the types described above are presented in figures 4A to E. Systems of type (A) with complete solubility in the solid and liquid phases are realized when both spe-

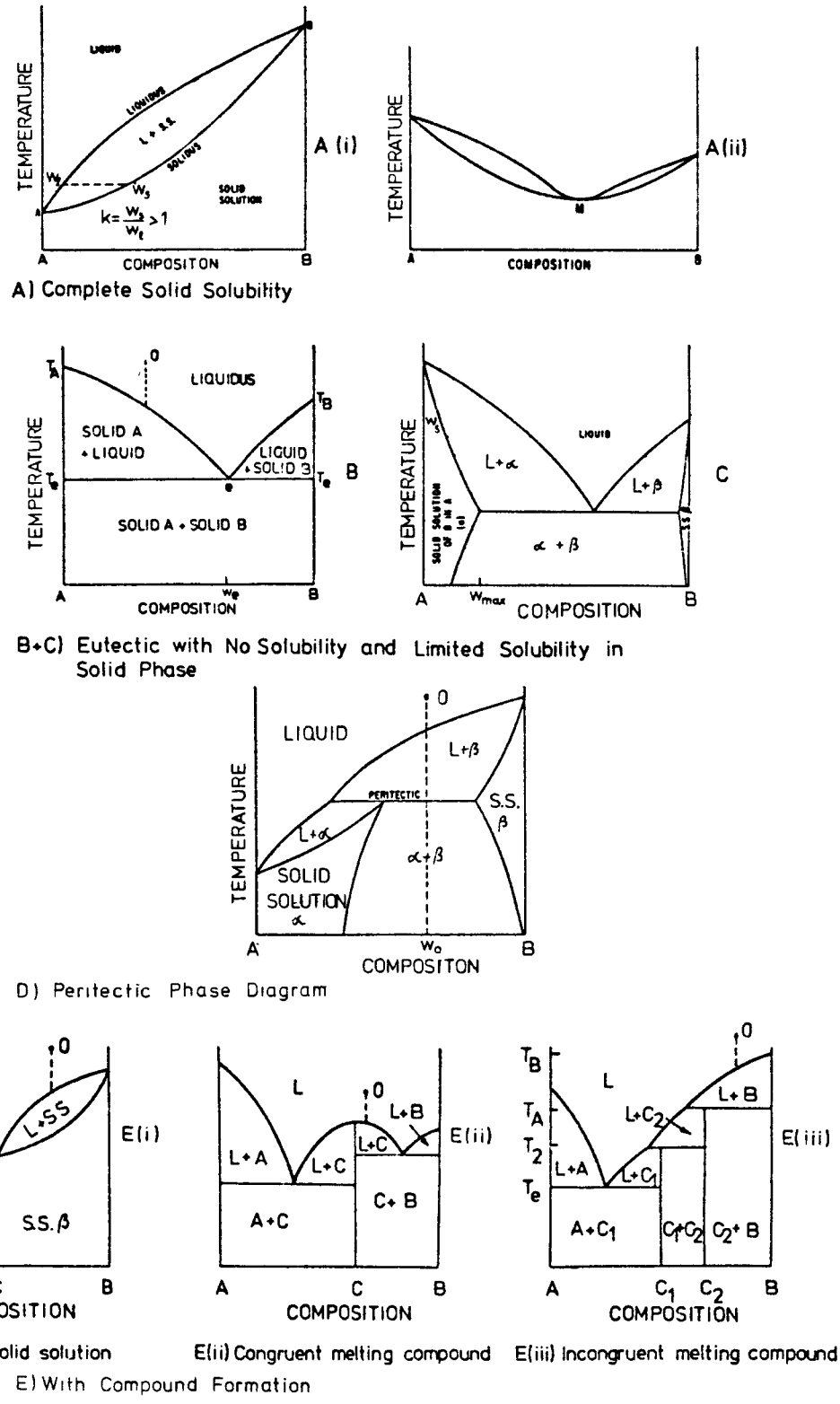

Fig. 4. — Phase diagrams [21].

cies are very similar in size and nature and when the crystals of both can accommodate each other. These types of systems are advantageous from the standpoint of reversibility of the melting and freezing processes. They, however, suffer from a large temperature range associated with phase change. The latter can of course be offset with the proper selection of the components, so that a minimum melting point M, as shown in figure 4A-(ii), exists. Since the melting and freezing points coincide at M, a mixture

of that composition will freeze and melt without segregation.

Simple eutectic systems of types (B) and (C) with no or limited solid phase solubility are also of particular interest due to the fixed melting and freezing points they possess. Systems of type (C), however, form additional phases α and β, which are homogeneous solid solutions of the component B in A and of the component A in B respectively.

Peritectic phase diagrams represented by figure 4D arise when B raises the freezing point of A but when there is only limited solid solubility. The characteristic of a peritectic reaction is that primary crystals β crystallized out of a solution react with the solution β to form a second phase α, i.e. $S + \beta \rightarrow \alpha$. Thus, if a mixture is cooled from point O the first solid to freeze out is solid solution β. Assuming no solid-state diffusion, the composition moves down the liquidus and past the peritectic temperature T_p. Below this temperature T_p, the solid solution α freezes out instead of β. The last liquid to freeze is pure A.

For systems of type (E) that form compounds, one distinguishes between systems wherein both components and the compound have complete solid solubility, and those in which there is no solid solubility. In the case of complete solubility, the phase diagram assumes the form shown in figure 4E-(i). Starting from the point O and assuming no solid-state diffusion, the last liquid to freeze out is pure compound C, so that the solidification is confined to the upper legs of the curves. With no solid solubility, the compounds formed can possess congruent or incongruent melting points, as shown in figure 4E-(ii) and (iii) respectively. If the compound has a congruent melting point, as in figure 4E-(ii), cooling from point O results in freezing pure compound C until the C-B point is reached in the liquid, at which time eutectic C-B freezes out till the liquid is gone. On the other hand, when a compound decomposes at its melting point, it is said to be incongruently melting. Figure 4E-(iii) is a phase diagram with two components C_1 and C_2 with incongruent melting points. If cooling is initiated from point O, pure B freezes out when the liquidus is reached. If the bulk solid is in equilibrium with bulk melt, the liquid freezes entirely at T_2. At this point, part of the liquid freezes out C_2 while a part combines with previously frozen B to yield solid C_2. On the other hand, if no solid-state diffusion occurs, the liquid composition follows the liquidus below T_2. From T_2 to T_1 pure C_2 freezes out. From T_1 to T_e pure C_1 freezes out. At T_e both A and C_1 solidify as a eutectic.

The understanding of phase diagrams can ease in the selection of phase change heat storage materials for use in LTES systems. As we shall see in chapter 4, the desired properties of suitable phase change materials are a narrow phase transition range, ability to melt congruently and without supercooling and stability to thermal cycling. In case the phase change materials are binary systems, it would be desired that they be of the type (A)-(ii) with a concentration that corresponds to the minimum melting temperature, or of types (B), (C) with a eutectic composition, or of type (E)-(ii) wherein the compounds formed have a congruent melting point.

A good example for the choice of a heat storage material is the $Zn(NO_3)_2$-H_2O system. Figure 5 shows the phase diagram for $Zn(NO_3)$-H_2O between the temperature limits -40 °C to $+80$ °C. If a liquid mixture of $Zn(NO_3)_2$ and H_2O is cooled below 80 °C, 5 different hydrated salts of $Zn(NO_3)_2$ shown in figure 5 crystallize out of solution. Of these, $Zn(NO_3)_2.9\,H_2O$ has an incongruent melting point while the remaining 4 hydrates have a congruent melting point. The 6-hydrate, with a melting point of 36.1 °C, additionally has a high latent heat of fusion and hence well-suited as a heat storage material.

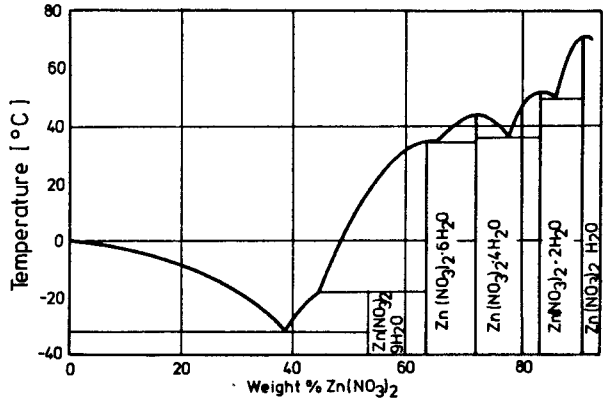

Fig. 5. — Phase diagram for $Zn(NO_3)_2$-H_2O system.

Another example that we wish to discuss here is the well-known storage material sodium sulphate-10-hydrate or Glauber salt. This material has been extensively investigated so far for use in LTES systems. Figure 6 shows a partial phase diagram of the sodium sulphate-water system [4]. $Na_2SO_4.10\,H_2O$ decomposes peritectically on heating to 32.4 °C to yield anhydrous sodium sulphate and a saturated solution of Na_2SO_4 in water. The solid crystals containing 44 % anhydrous Na_2SO_4 and 56 % water by weight change to a mixture of 15 % anhydrous Na_2SO_4 and 85 % saturated solution of Na_2SO_4 in water (10 H_2O). The 15 % anhydrous Na_2SO_4 remains insoluble and settles down as a white bottom sediment. It is not possible to dissolve this material by the usual expedient of increasing the temperature, because the highest solubility occurs at the melting point with solubility decreasing at higher temperatures. Due to the large density difference between the saturated solution (1 350 kg/m^3) and the anhydrous solid Na_2SO_4 (2 650 kg/m^3), gravity induced separation results. Consequently melting is partly incongruent due to segregation [18].

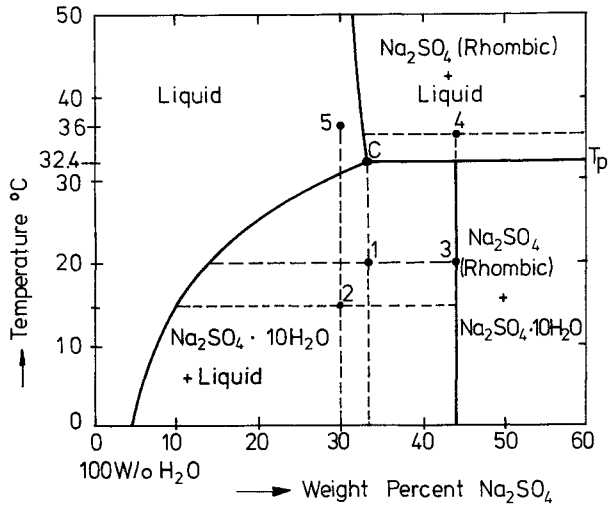

Fig. 6. — Partial phase diagram for Na_2SO_4-H_2O system [4].

Now, if the mixture of the saturated solution and anhydrous salt is cooled below 32.4 °C, sodium sulphate can be absorbed in the solution only as rapidly as water can diffuse through solid sodium sulphate decahydrate to the anhydrous sodium sulphate particles, on which the decahydrate particles form. Since peritectic solidification reactions are characteristically much slower than congruent solidification or eutectic solidification, and because the rate limiting process here is solid state diffusion, even stirring cannot significantly effect the rate of absorption of Na_2SO_4, which therefore collects at the bottom of the container.

If the phase diagram for the Na_2SO_4-H_2O system is now carefully followed, it can be seen that the solid state diffusion as a reaction step can be eliminated by using a mixture of decahydrate and water as the starting material (68.2 % $Na_2SO_4.10\,H_2O$ and 31.8 % H_2O by weight). At 15 °C (point 2) this mixture consists of 58.1 % $Na_2SO_4.10\,H_2O$ and 41.9 % solution of composition 10.6 % Na_2SO_4 and 89.4 % H_2O by weight. When the temperature of the mixture is raised, the solubility of decahydrate increases with the increase in temperature [4].

With the composition chosen, all the decahydrate dissolves when the system is heated above 32 °C and no segregation hence takes place. The overall composition of the solution then is 30 % Na_2SO_4 and 70 % H_2O by weight. Now if the solution is cooled from 36 °C (point 5 in figure 7), decahydrate crystals should begin to separate, as the solution reaches the liquidus line (at 30 °C). With further reduction in temperature, the system enters into a two-phase region, $Na_2SO_4.10\,H_2O$ and liquid. The amount of each constituent can be easily calculated at any temperature by using the Lever rule. The stored thermal energy in the system is released when the $Na_2SO_4.10\,H_2O$ crystals separate from the solution.

2.2.2 *Supercooling of the melt and nucleation.* — We have stated earlier that for crystallization of the liquid to occur, nuclei must form and grow. In fact, the phase diagrams described above assume that nuclei exist in the melt and cause crystallization to occur at the thermodynamic freezing point. A melt is said to be supercooled if its temperature is below the freezing point and no crystals have appeared within it.

Most inorganic salt hydrates, that qualify as phase change heat storage materials due to other favourable properties, tend to supercool. It has widely been mentioned in the literature that suitable nucleating agents must be added to them to promote the formation of crystals at the freezing point of the materials. In this section we hence wish to examine the theory of nucleation and the supercooling of a melt.

2.2.2.1 Homogeneous nucleation. — Homogeneous nucleation implies the formation of solid nuclei in a bulk liquid in the absence of a solid substrate contacting the liquid [9, 17].

Consider a spherical solid nucleus of radius r within a liquid maintained at its melting temperature T_M. For the crystal to exist in the liquid, its temperature T must be below T_M and the free energy $G_{V,S}$ per unit volume of the solid nucleus is below the corresponding free energy $G_{V,L}$ of the melt. The difference in free energies $\Delta G_V = G_{V,L} - G_{V,S}$ is the driving force for the crystal formation and, as a first approximation, is proportional to the Supercooling $\Delta T = T_M - T$, i.e. $\Delta G_V = \alpha\,\Delta T$. This driving force most overcome the surface energy required to maintain the interface between the solid nucleus and the surrounding liquid.

The total change in free energies between the two phases is hence given by [9]

$$\Delta G_{total} = \begin{pmatrix}\text{difference in}\\ \text{free energies}\end{pmatrix} + \begin{pmatrix}\text{interfacial}\\ \text{energy}\end{pmatrix}$$

or

$$\Delta G_{total} = -\,\Delta G_V . \tfrac{4}{3}\pi r^3 + \gamma . 4\pi r^2 \qquad (4)$$

where γ is the specific interfacial energy per unit area. ΔG_{total} is also a measure of the work required for crystal formation.

The three functions contained in equation (4) are depicted graphically in figure 7. The total change in

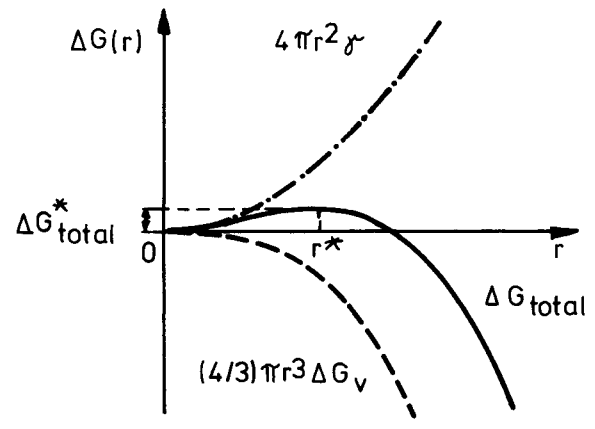

Fig. 7. — Free energy contributions towards the formation of a solid nucleus [9].

free energies ΔG_{total} is seen to exhibit a maximum for a nucleus of radius r^*. The magnitude of r^* is found by putting $\frac{d}{dr}(\Delta G_{total}) = 0$.

Hence,

$$r^* = \frac{2\gamma}{\Delta G_V}. \quad (5)$$

Substituting for $\Delta G_V = \alpha.\Delta T$

$$r^* = \frac{2\gamma}{\alpha.\Delta T}. \quad (6)$$

Using the above value of r^* in equation (4)

$$\Delta G^*_{total} = \frac{16\pi\gamma^3}{3(\Delta G_V)^2} = \frac{16\pi\gamma^3}{3.\alpha^2.\Delta T^2} \quad \text{at} \quad r = r^*. \quad (7)$$

The radius r^* is called the critical radius and is inversely proportional to the supercooling ΔT, i.e. larger the supercooling, smaller would be the critical radius. All nuclei of radii $r < r^*$ are thermodynamically unstable, while nuclei of radii $r > r^*$ grow with gain in energy.

A common question that arises is : How large should the supercooling be to form a stable solid nucleus. From statistical thermodynamics, we introduce the relationship between the Boltzmann factor and the energy change ΔG^*_{total} as [9]

$$N^* = N \exp(-\Delta G^*_{total}/kT) \quad (8)$$

where N^* is the probable number of critical nuclei per N atoms in the melt at temperature T. For $N^* = 1$, the critical supercooling ΔT_{Cr} is then obtained from equations (7) and (8) as,

$$\frac{\Delta T_{Cr}}{T_M} = \left[\frac{16.\pi.\gamma^3}{3\,T_M^2\,\alpha^2\,kT \ln N}\right]^{1/2}. \quad (9)$$

The factor α may be determined by writing the Gibbs free energy ΔG_V in terms of the heat of fusion L_F and entropy S.

Thus

$$\Delta G_V = L_F - T.\Delta S. \quad (10)$$

At the melting point T_M, $\Delta G_V = 0$, so that

$$\Delta S = L_F/T_M.$$

Substituting for ΔS in equation (10)

$$\Delta G_V = \frac{L_F(T_M - T)}{T_M} = \frac{L_F.\Delta T}{T_M}$$

or

$$\alpha = \frac{\Delta G_V}{\Delta T} = \frac{L_F}{T_M}.$$

Using the above value of α in equations (6) and (7), we have,

$$r^* = \frac{2\gamma T_M}{L_F\,\Delta T} \quad (11)$$

and

$$\Delta G^*_{total} = \frac{16\pi\gamma^3\,T_M^2}{3\,L_F^2\,\Delta T^2} \quad (12)$$

where $\Delta T = (T_M - T)$ is the amount of supercooling.

Unfortunately, the value of γ is not known theoretically and must be deduced from experimental data for T_{Cr}/T_M.

2.2.2.2 Heterogeneous nucleation. — By heterogeneous nucleation of a crystal from a melt, we understand nucleation from the surface of foreign bodies present in the melt. Such foreign bodies may be in the form of a solid substrate, or crystals of some other substance, e.g. nucleating agents, or even dust and dirt particles. It is now well known from experimental observations that heterogeneous nucleation requires a much smaller critical supercooling ΔT_{Cr} for the formation of solid nuclei [9, 17].

An example of heterogeneous nucleation is the nucleus formation on a wall, as seen in figure 8. A nucleus of critical radius r^* now occupies a much smaller volume which further reduces as the contact angle decreases. The contact angle itself can be determined by a force balance of the interfacial tensions between the solid (S) and liquid (L) phases and the wall or substrate (W). Thereby,

$$\sigma_{SL} \cos\theta = \sigma_{LW} - \sigma_{SW}.$$

Due to a smaller nucleus volume, the work required to form the crystal ΔG_{total} and the supercooling ΔT are also small.

The substrate hence acts as a catalyst that promotes nuclei formation during crystallization at smaller supercooling of the melt. The effectiveness of the substrate, however, depends on the coherence of its crystal lattice structure with that of the solid nucleus, its chemical nature and its topography [9]. These factors must hence be borne in mind during the choice of nucleating agents to promote crystal formation in phase change heat storage materials for LTES systems.

The determination of proper nucleating agents is

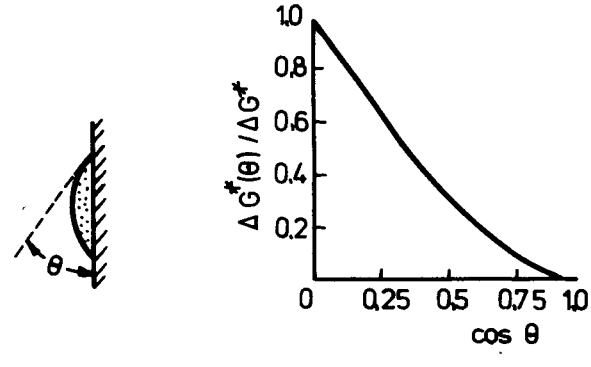

Fig. 8. — (*a*) Nucleation on a wall. (*b*) Relationship between the work required to form a crystal during homogeneous and heterogeneous nucleation as a function of contact angle [9].

often time consuming and is said to involve more luck and art than science [12]. Therefore, only a few nucleating agents for storage materials are presently commonly known. The most common ones are 3-5 % Borax (sodium tetraborate decahydrate) for $Na_2SO_4.10\ H_2O$ [20] and 1 % ZnO and $Zn(OH)_2$ for $Zn(NO_3)_2.6\ H_2O$ [12].

3. **Sensible heat thermal energy storage.** — 3.1 HEAT STORAGE IN WATER. — Water is the most widely used heat storage medium to store low temperature solar heat today. In several cases, water serves simultaneously as the heat storage medium and the heat transfer medium. Thus for most applications, load side heat exchangers may be eliminated. Particularly in the case of domestic hot water systems, the storage is generally hooked on directly to the water pipe line, whereby hot water is withdrawn from the top of the tank and is replaced by an equivalent amount of cold water from the pipe line introduced at the bottom of the tank.

Most current research on water storage tanks is aimed at the development of economical, efficient and durable systems for storing solar heat in water and at understanding the role played by stratification in the water tanks on the performance of the solar heating system. Our discussion in the present paper shall hence be addressed to these two major points of interest.

3.2 REQUIREMENTS FOR HOT WATER STORAGE SUBSYSTEMS. — The requirements for hot water storage subsystems have been summarized well by Pickering [15] and shall be reproduced here.

1) *Function* : The application concerned, e.g. hot water production, space heating, space cooling, etc., has an important bearing on the shape, size, location, requirements, etc., of the water storage tank.

2) *Capacity* : The capacity varies between 300 l to 500 l for the domestic hot water requirements for a 4-person household, and between 2 000 l and 10 000 l for single-family residences. The right choice of the tank size must be determined through system simulation study, and depends on a number of diverse factors, such as insolation, load, overall system efficiency, amount of load to be covered by solar, etc.

3) *Temperature capability* : Typical storage temperatures are 40-80 °C for domestic hot water, 60-80 °C for space heating and 90-95 °C for space cooling or solar system combinations that include cooling.

4) *Durability* : Corrosion, heat and chemical deterioration and insulation degradation due to water and vapor infiltration affect durability. Minimum storage life is suggested to be 10 years if subsystem is readily repairable or replaceable, 20 years minimum life if this is not the case.

5) *Interface capability* : The subsystem must permit ready interface for the attachment or integration of input and output lines, heat exchangers, vents, valves, drains, instruments, etc.

6) *Safety and health* : The subsystem must be safe from catastrophic flooding, must be capable of being fully drained by gravity if heated in interior spaces and must be protected by suitable air gaps or back-flow devices to prevent cross-connection with the domestic water system.

7) *Integration with structure* : The subsystem must be capable of integration with residential structures without undue space requirements and infringement on living space and aesthetic values.

8) *Access* : Ready accessibility for adjustment, cleaning, repairs, etc., must be provided. Man space will generally be required.

9) *Repairability* : The subsystem must be readily repairable with minimum skills.

10) *Replaceability* : The subsystem must be easily replaceable at the end of its service life.

11) *Heat retention* : The subsystem must prove its capability of heat retention in the storage water during the system life. Thus the insulation must not degrade with time. This is particularly important for underground subsystems, where the insulation must be protected by appropriate waterproofing measures to prevent waterlogging.

12) *Flexibility* : The subsystem must retain flexibility for future changes in insulation, capacity, etc.

3.3 TYPE OF STORAGE TANKS. — Steel, aluminum, concrete and plastics, sometimes also wood, are generally considered as construction materials for hot water storage tanks. In the case of metallic tanks, vertical tanks are generally preferred in comparison to the horizontally mounted ones because of the requirement of the latter to resist beam bending and buckling action. In case the tanks are located below ground adequate protection against corrosion must be observed. Interior corrosion protection would also require coatings of some sort, for example galvanizing of steel tanks, or coating with plastic paint-like products, or rubber-like sheet materials such as neoprene, butyl rubber, etc. [15].

Concrete as a container material for tanks is now also widely used. A variety of tank forms are available. Thermal expansion problems, however, require careful design and some additional reinforcing material than for the constant temperature applications may be needed. If properly designed, concrete tanks need not be lined. Low quality, precast vessel should, however, be lined, as cracking due to thermal expansion will invariably occur.

Fiberglass-reinforced plastic tanks offer a major advantage in that they are corrosion resistant. Both horizontal underground storage tanks and vertical overground tanks are available.

Through the use of suitable polyester resins and polymers, operating temperatures upto 95 °C may

be used. Polyurethane foam is the common insulation employed ; in the case of the underground tanks, coal tar or asphalt waterproof coating is additionally used. Considerable experience with fiberglass tanks filled with oil exists today and their durability has been to a large extent proved [15].

3.4 STRATIFICATION IN SOLAR WATER HEAT STORAGE TANKS. — Thermal stratification implies the existence of *temperature-layers* within a water storage, whereby the hot and cold water layers are separated by an invisible sheet of water. Stratification is achieved through the elimination of mixing during storage, whereby a two-fold advantage is gained [16] : (1) The efficiency with which the energy can be used will be improved if it is supplied to the load at the temperature it was collected rather than at a lower mixed-storage temperature ; (2) the amount of energy collected may be increased if the collector inlet fluid temperature is lower than the mixed-storage temperature. The absolute and relative importance of either of these effects shall, of course, depend on the solar system design and the intended application.

For a typical residential space heating system, as shown in figure 9, Sharp and Loehrke [16] have recently carried out a detailed investigation of the system performance when stratified water storage is employed. In their study, they investigated the influence of a large number of parameters, such as number of tank segments used to modell stratification, collector mass flow rate, collector efficiency, building loss coefficient, storage tank volume, tank height-to-diameter ratio, partial stratification effects, etc. Hourly weather data for seven days in January in Boulder, Colorado were used as input to their simulation analysis. Their results showed that an improved performance results if stratification can be achieved in the storage tank. For the various parameters considered, the benefit due to stratification, as measured by the increase in the fraction of the total heating load supplied by solar energy, ranged from about 5 to 15 %.

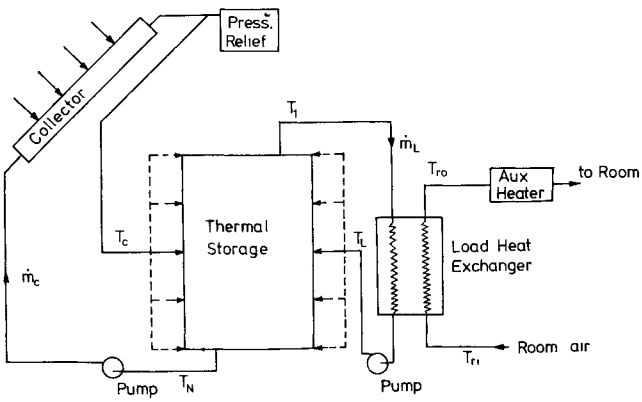

Fig. 9. — Schematic of a typical residential space heating system employing a stratified water storage subsystem [16].

Measurements on a solar hot water heating system for a 10-unit apartment complex (collector area = 34 m^2) using a 1 700 l stratified hot water storage tank have been reported under Projekt SAGE [5]. Typical temperature profiles showing the charging and discharging of the storage over a 24-hour period are shown in figure 10. Measurements showed that an approximately 0.3 m thick thermocline is established in the tank as hot water is withdrawn from the tank. The storage is fully charged at 16.00 hours, i.e. at the end of the day's solar energy input period. The total improvement in system performance was found to be on the order of 10 % when a stratified water tank was used.

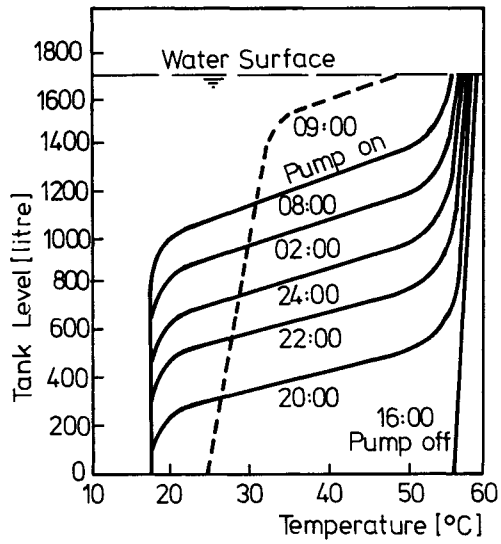

Fig. 10. — Temperature distribution in a stratified water storage [5].

4. **Latent heat thermal energy storage (LTES).** — Any latent heat thermal energy storage system must possess at least the following three components :

1) a heat storage substance that undergoes a solid-to-liquid phase transition in the operating range and wherein the bulk of the heat added is stored as the latent heat of fusion ;

2) a containment for the storage substance, and

3) a heat exchanging surface for transferring heat from the heat source to the heat storage substance and from the latter to the heat sink, e.g. from the solar collector to the heat storage substance to the load loop.

The development of a latent heat thermal energy storage (LTES) system hence involves the understanding of two essentially diverse subjects : heat storage materials and heat exchangers. The flowchart in figure 11 provides an overview of the different stages

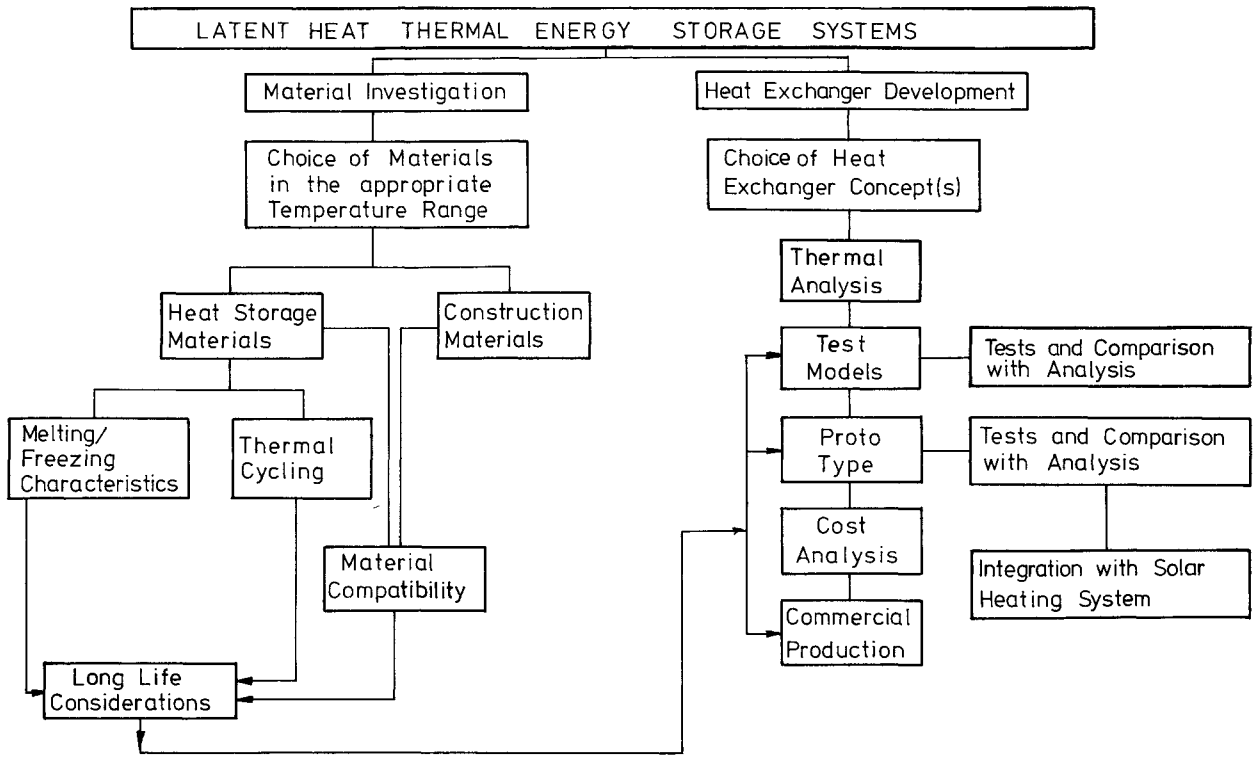

Fig. 11. — Flowchart showing the development of a latent heat thermal energy storage system.

that may be involved in the development of a LTES system and of the specialized problems that need to the tackled. The problems concerning materials and heat exchangers are discussed in greater detail in sections 4.1 and 4.2.

4.1 PHASE CHANGE HEAT STORAGE MATERIALS. — 4.1.1 *Desired material properties.* — A large number of organic and inorganic substances are known to melt with a high heat of fusion in any required temperature range, e.g. 20-80 °C. However, for their employment as heat storage materials in LTES systems, these phase change materials must exhibit certain desirable thermodynamic, kinetic and chemical properties. Moreover, economic considerations of cost and large-scale availability of the materials must be considered. The various criteria that govern the selection of phase change heat storage materials are summed in table III below [14].

4.1.2 *Candidate heat storage materials.* — It is quite apparent that no single material can fully satisfy the long list of criteria listed in table III. Trade-offs are hence made in the selection of candidate phase change heat storage materials in a desired operating temperature range. Within the operating temperature range of 20-80 °C, candidate phase change heat storage materials are grouped into the families of organic and inorganic compounds and their eutectica, as seen in figure 12. Sub-families of organic compounds include paraffin and non-paraffin organics.

Figures 13*a* and *b* respectively show the latent heat

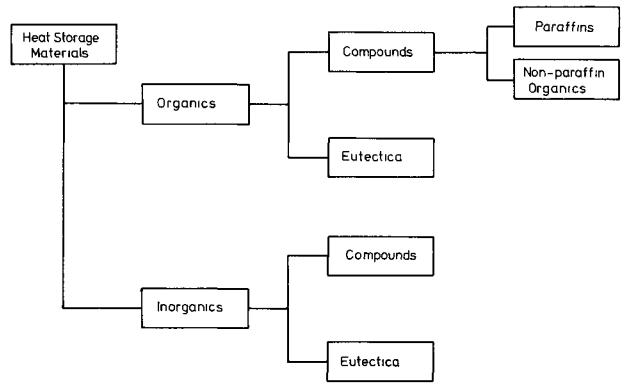

Fig. 12. — Families of phase change heat storage materials.

of fusion per unit mass and per unit volume of some phase change heat storage materials of interest in the temperature range 20-80 °C [1]. Of particular interest is figure 13*b*, which provides information on the compactness of a LTES system for a given amount of energy storage. Figure 13*b* further shows that while the inorganic salts possess relatively large heats of fusion, their melting points generally lie below 40 °C. Organic compounds, on the other hand, have melting points spread over a large temperature range but possess a smaller heat storage capacity, e.g. their storage capacity per unit volume is in the order of 150-200 MJ/m^3, about one-half that of inorganic salts.

Not withstanding the disadvantages concerning

Table III. — *Desired properties of phase change heat storage materials* [14].

A) *Thermodynamic criteria*

The phase change material should possess :

- a melting point in the desired operating temperature range
- high latent heat of fusion per unit mass, so that a lesser amount of material stores a given amount of energy
- high density, so that a smaller container volume holds the material
- high specific heat to provide for additional significant sensible heat storage effects
- high thermal conductivity, so that the temperature gradients required for charging and discharging the storage material are small
- congruent melting : the material should melt completely so that the liquid and solid phases are identical in composition. Otherwise, the difference in densities between solid and liquid will cause segregation resulting in changes in the chemical composition of the material
- small volume changes during phase transition, so that a simple containment and heat exchanger geometry can be used.

B) *Kinetic criteria*

The phase change material should exhibit :

- little or no supercooling during freezing. The melt should crystallize at its thermodynamic freezing point. This is achieved through a high rate of nucleation and growth rate of the crystals. At times, the supercooling may be suppressed by introducing nucleating agents or a *cold finger* in the storage material.

C) *Chemical criteria*

The phase change material should show :

- chemical stability
- no chemical decomposition, so that a high LTES system life is assured
- non-corrosiveness to construction materials
- the material should be non-poisonous, non-flammable and non-explosive.

D) *Economic criteria*

The phase change material should be :

- available in large quantities
- inexpensive.

volume requirements, the organic substances serve as important heat storage materials due to the several desirable properties they possess in comparison with inorganic compounds. Some of these advantages includes their ability to melt congruently, their self-nucleating properties and their capability to freeze without supercooling, and their compatibility with conventional materials of construction.

4.1.3 *Melting and freezing characteristics.* — By melting and freezing characteristics of phase change heat storage materials, we understand the behaviour exhibited by these materials during heating and cooling, e.g. melting and freezing ranges, congruency of melting, nucleation characteristics, supercooling of the melt and stability to thermal cycling. All these factors are of extreme importance to the life of a LTES system and shall now be discussed here.

4.1.3.1 Typical heating and cooling curves. — The heating and cooling curves are generally traced using samples of the phase change materials in a Differential Thermal Analyzer (DTA) or in sealed glass containers, e.g. test tubes or bottles. At times, these curves are also obtained in testmodels of actual LTES systems. The three methods distinguish themselves in terms of the quantity of the sample and the speed with which results can be obtained. For example, the DTA provides quick and reliable results using very small quantities of the sample (ca. 1-10 mg). The DTA is, however, a severe test for phase change materials that supercool, since the supercooling tendencies are maximized due to the small weight of the samples. Tests in glass containers, on the other hand, use about 10-100 g for the material and are hence slower. With proper care, the rate of heating and cooling can be well controlled and relatively accurate results can be gained. The tests in glass containers, however, suffer from the disadvantage that metallic surfaces that generally form the heat exchanging surface within a latent heat store are absent. Nucleating conditions different to those in actual LTES systems hence exist. Experiments done in testmodels are the most accurate of all as conditions similar to those in large-scale LTES systems are simulated within them. These tests are also the slowest in comparison to the other techniques due to the large quantities of phase change material they require (1-10 kg).

Figures 14 and 15 show typical heating and cooling curves for three different groups of phase change materials — paraffin organics, non-paraffin organics and inorganic salt hydrates [10]. The materials represented in these diagrams are paraffin C16-C18 (a paraffin mixture), lauric acid (a fatty acid) and sodiumhydrogenphosphate-12-hydrate. The temperatures at the beginning and end of melting and freezing are obtained by analysing the slopes of the heating and cooling curves and their values are presented in table IV along with the melting range recommended by the manufacturer of the material.

The values in table IV indicate a discrepancy between the melting and freezing ranges for the two organic substances. In general, the cooling curves provide more accurate information and these should hence be considered for data evaluation.

A number of interesting observations may be made from figures 14, 15 and from the results in table IV.

1. *Paraffin.* — Paraffin exhibits two freezing ranges : a narrow freezing range existing for a short period of time and a larger freezing range that occurs for a longer period of time. The two freezing ranges are respectively considered to signify a liquid-to-amorphous solid transition and an amorphous-solid-to-crystalline solid transition. A part of the total latent heat of fusion is stored in the substance during each of these transitions.

Not all commercially available paraffins (all of

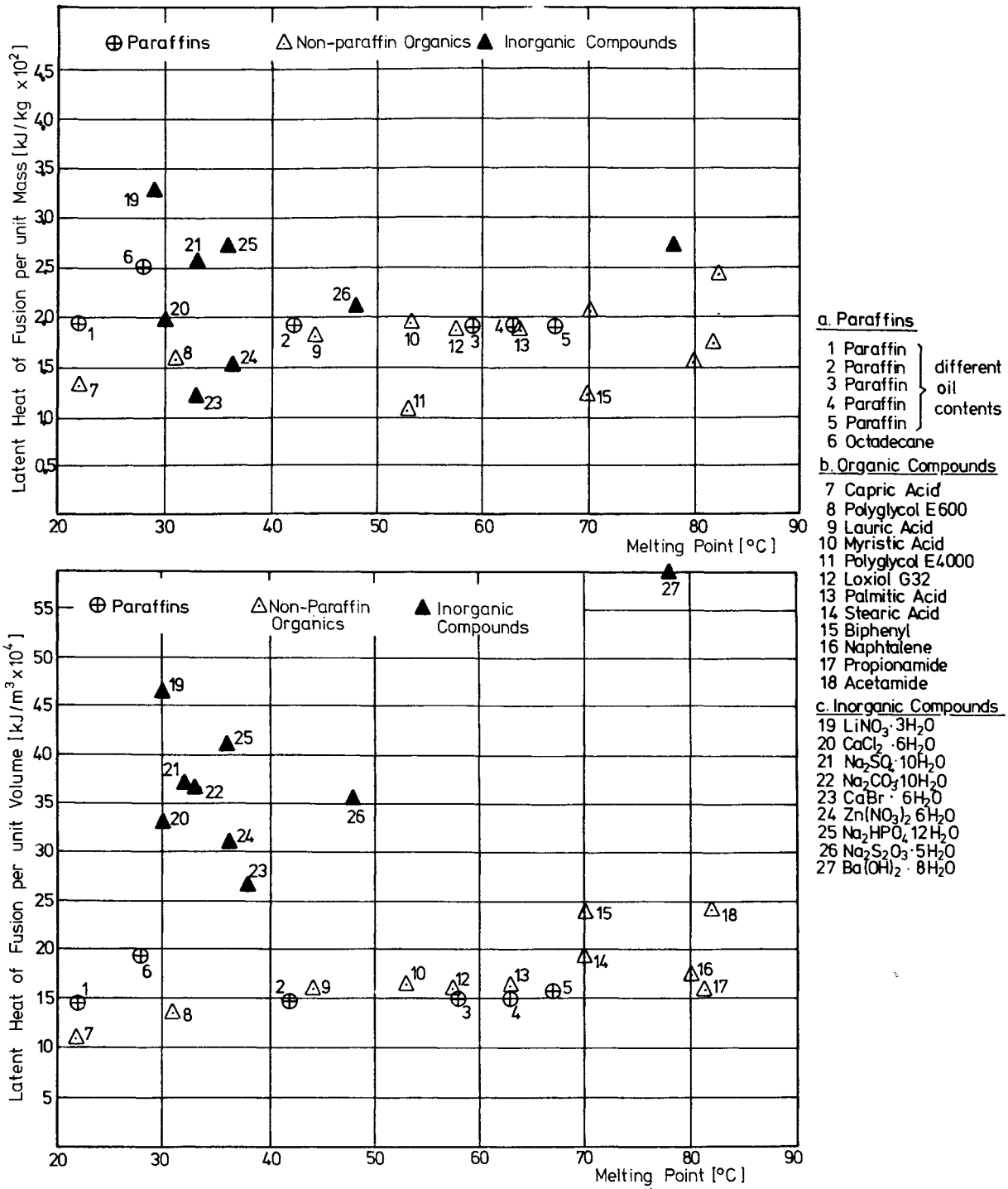

Fig. 13(*a*), (*b*). — Latent heat of fusion per unit mass and per unit volume of selected phase change heat storage materials in the temperature range 20-80 °C [1].

Table IV. — *Melting and freezing ranges of selected heat storage materials.*

Phase change heat storage material	Manufacturer's recommended melting/freezing range (°C)	Experimentally observed melting range (°C)	Experimentally observed Freezing range (°C)	Supercooling (K)
Paraffin	42-44	36-43	38-43	—
Lauric acid	42-44	40-43	42-43	0.5
$Na_2HPO_4.12\ H_2O$	36	36	36	10.5

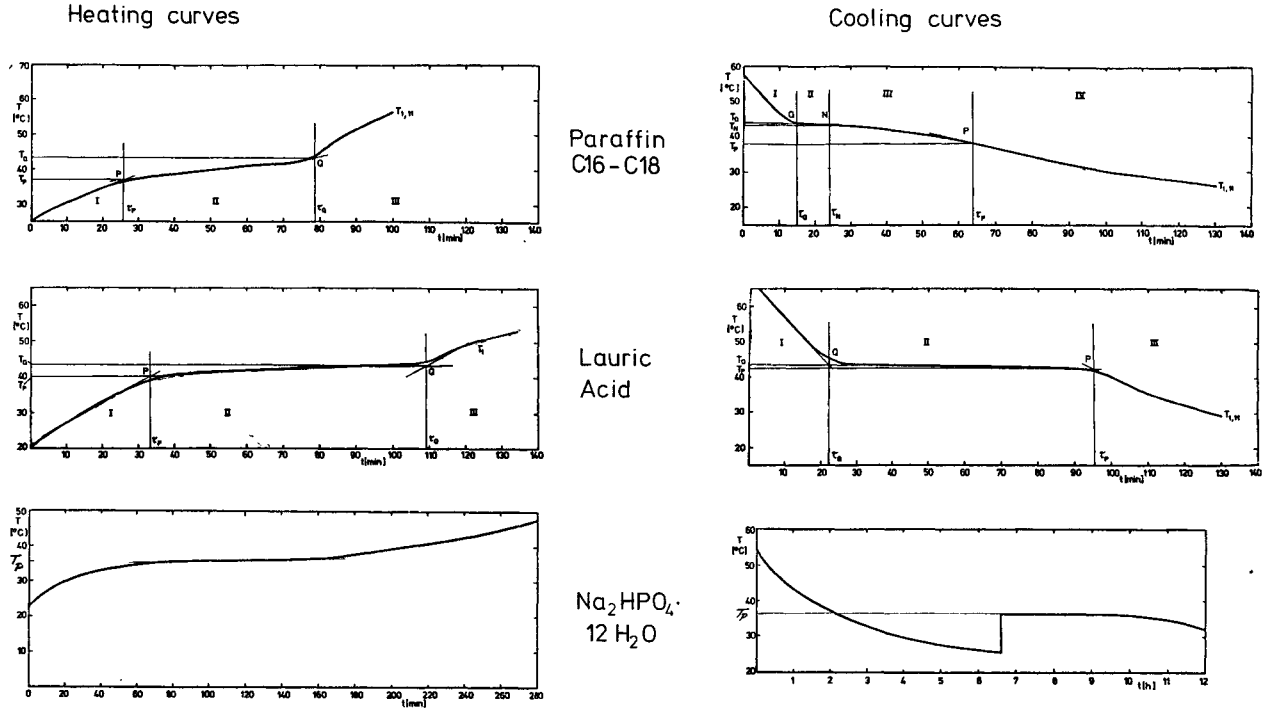

Fig. 14. — Typical heating curves for paraffin organics, non-paraffin organics and inorganic salt-hydrates.

Fig. 15. — Typical cooling curves for paraffin organics, non-paraffin organics and inorganic salt-hydrates.

these are essentially paraffin mixtures) display a freezing behaviour as shown in figure 14. For the sake of comparison the cooling curves for three different paraffins are presented in figure 16. The paraffins in this diagram vary extensively in their freezing interval which is bounded by the points marked Q and P on the diagram, which signify the beginning and the end of the freezing process. Sample No. 2 with 4 % oil content, for example, has too large a freezing interval which renders it completely unfit for use in a LTES system. In fact, the point P marking the end of freezing can hardly be determined for this paraffin.

A final important observation with paraffin is the large difference between the experimentally measured freezing range and the manufacturer's data. This result is of particular importance to the design and operation of a LTES system, which calls for an exact knowledge of the phase transition temperature range of the heat storage material.

2. *Lauric acid.* — Lauric acid, a fatty acid, exhibits excellent melting/freezing characteristics. The freezing plateaus are long and flat and no supercooling is evident, though in some cases, a small degree of supercooling ($\sim$ 0.5 K) has been measured. This behaviour is representative of all fatty acids and also of polyethylene glycols with melting points between 15 °C and 70 °C [12]. These materials have, however, not yet received special favour for use in LTES systems due to their higher cost.

3. *Inorganic salt hydrate.* — The freezing curve of sodiumhydrogenphosphate-12-hydrate is typical of

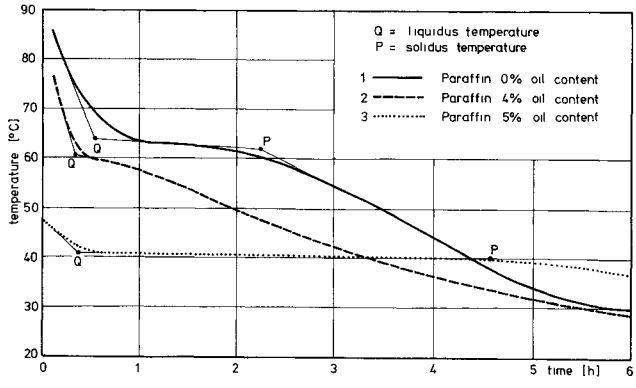

Fig. 16. — Comparison of cooling curves for 3 different paraffins [10].

most hydrate salts in the temperature range 20-80 °C. Freezing curves for several other salts [19] are presented in figure 17. For all these materials the melt does not freeze at its thermodynamic freezing point, but is supercooled by several degrees below the freezing point. The supercooled liquid hence exists in a highly metastable state. Formation or introduction of a single crystal nucleus into the melt causes a spontaneous crystallization of the whole melt.

Most attention so far has been devoted to the study of inorganic salt hydrates as phase change heat storage materials, primarily due to their low cost and their ability to store large amounts of heat per unit volume, in comparison to the organics. Several studies have concentrated on the search of nucleation agents that are added in minor quantities

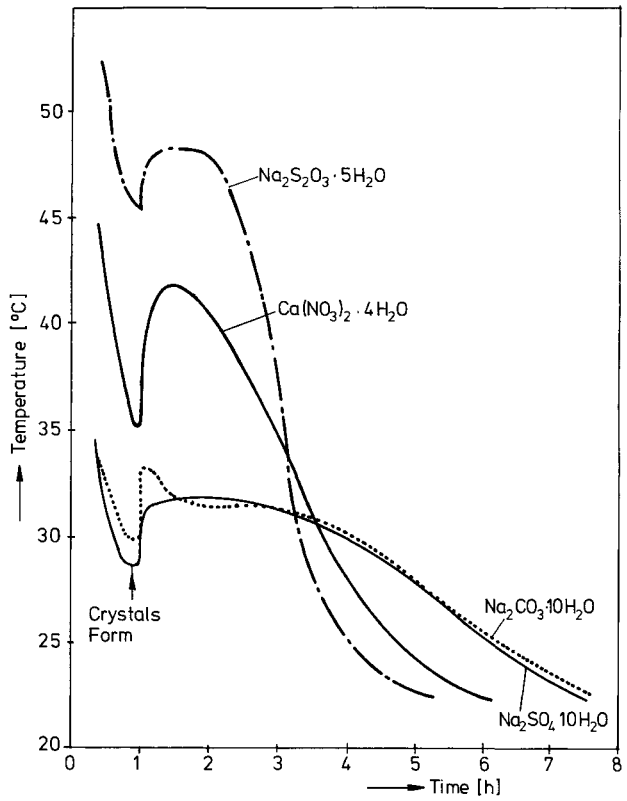

Fig. 17. — Comparison of cooling curves for salt-hydrates [19].

to the parent material in order to promote crystal nucleation in the melt and hence to eliminate supercooling. Techniques for encapsulation of the salt hydrates have been developed, whereby emulsion-sized particles, or granules, or even large blocks of the materials are encapsulated in flexible polyester resins. None of these techniques, however, has so far attained a stage of full reliability and a great amount of further research is required before the inorganic salt hydrates can successfully be put to use.

4.1.3.2 Thermal cycling. — One of the most severe tests that phase change heat storage materials must undergo is thermal cycling involving repeated melting and freezing of the heat storage materials. For example, for a 20 year life of a one-day storage, the phase change material experiences one melting-freezing cycle daily or a total of 7 365 cycles during the system life.

The influence of thermal cycling on the phase change material characteristics must be measured experimentally. A large gap exists today in this area. Limited thermal cycling (120 cycles) carried out with paraffins and lauric acid exhibited no degradation of materials [10]. Test results for 1 000 heating-cooling cycles with $Na_2SO_4.10\,H_2O$ are also available [20]. Two material samples of $Na_2SO_4.10\,H_2O$ were used in these tests — one sample comprising the phase change material and 3 % Borax by weight as nucleating agent, and the second sample comprising the same constituents as above plus 8 % thickener that formed a thioxtropic gel. The results of these thermal cycling tests are presented in figure 16. The material with thickener showed no degradation in properties following cycling. However, the material without the thickener contained approximately 30 to 35 % liquid at the end of the cooling cycle. A sediment layer formed which remained throughout the testing period. The non-thickened material is also seen in figure 16 to reach a higher temperature during its heating cycle, due to the unavailability of the stratified lower layer.

Limited thermal cycling (upto 90 cycles) of $Na_2HPO_4.12\,H_2O$ showed that the material melts congruently when it is not contaminated with the heptahydrate, i.e. when the formation of the heptahydrate has been prevented by appropriate nucleation [20].

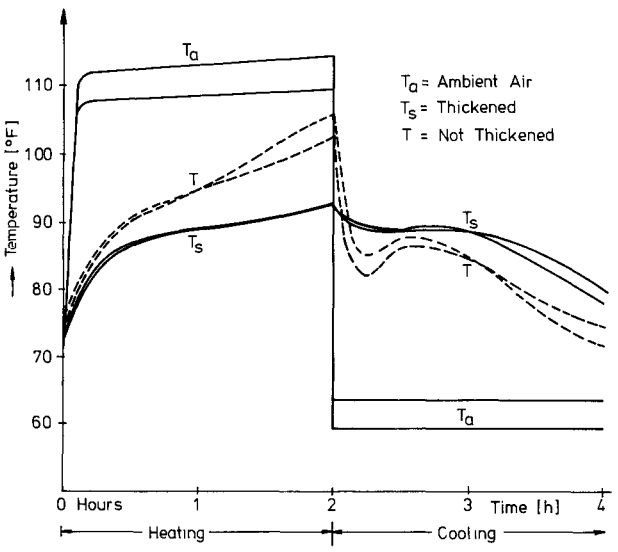

Fig. 18. — Thermal cycling tests for $Na_2SO_4.10\,H_2O$ [20].

4.1.4 *Compatibility with materials of construction.* — Knowledge regarding the compatibility of phase change heat storage materials with conventional materials of construction is of particular importance to the assurance of the life of a LTES system. Only limited compatibility data is presently available and the results reported here are those gained from some recently conducted tests [10, 11].

Figure 19 shows the combinations of the phase change materials and metals, which were subjected to experiments. Metal samples having dimensions of 30 × 25 × 2 mm were cleaned and wetpolished with 1 000 grain abrasive paper. The samples were immersed in the liquid phase of the storage material contained in air-tight bottles, one sample to a bottle. The bottles were placed in a thermostatically controlled water bath, whose temperature was maintained constant at 20 K above the melting point of the corresponding storage material.

Heat Storage Material \ Metal	Al 99,5	AlMg 3	Cu 99,9	Stainless Steel 1.4301	Mild Steel 1.0330
Sodiumthiosulphate-5-hydrate (48°C)*	x	x	x	x	x
Sodiumhydrogenphosphate-12-hydrate (35°C)	x	x	x	x	x
Calciumchloride-6-hydrate (30°C)	x	x	x	x	x
Loxiol G32 (58°C)		x	x	x	
Lauric acid (44°C)		x	x	x	

* melting point in brackets

Fig. 19. — Heat storage materials and materials of construction selected for the corrosion investigations.

The metal samples were removed from the bottles after predetermined time intervals and cleaned. Gravimetric analysis prior to and following the corrosion tests provided the mass loss Δm (g). Using DIN 50905, the reduction in sample thickness Δs (μm) and the corrosion rate v ($g\,m^{-2}\,d^{-1}$) or (mm/a) were then computed. Measurements were carried out using various samples of the same metal, which were in contact with the same storage material for different periods of time. Information on the temporal variation of the corrosion behaviour could thus be obtained. In accordance with Dechema tables [6], a metal experiencing a thickness reduction of $\leqslant 0.1$ mm/a was then termed corrosion resistant, and of $\leqslant 1.0$ mm/a fairly corrosion resistant. For cases where the corrosion rate attained a linear value, an estimate of the lifetime was possible.

In addition to the gravimetric analysis, optical and scanning electron microscopy techniques were employed to investigate the sample surface and cross-sections. The products of corrosion were furthermore chemically analysed.

The results of these investigations are summed up in table V. The organic materials were found to be compatible with the metals tested. With the salts, however, one needs to be careful as preferential compatibility was observed. Stainless steel is the only metal that was found compatible with all phase change materials tested. Copper exhibited rapid corrosion when immersed in sodiumthiosulphate-5-hydrate and a black layer of CuS was seen to form just 10 days after contact. The mass loss of the sample after 300 days of contact was found to be 8.17 g and the thickness reduction 610 μm. A photograph of the corroded sample taken after 50 days contact is presented in figure 20.

Fig. 20. — Surface of Cu 99.9 sample after 50 d in $Na_2S_2O_3.5\,H_2O$.

Aluminum and aluminum alloy $AlMg_3$ were found incompatible with sodiumhydrogenphosphate-12-hydrate and were covered with a white layer of aluminum hydroxide $Al(OH)_3$ after a short period

Table V. — *Results of corrosion investigations* [10, 11].

Heat storage material \ Metal	Al 99.5	AlMg 3	Cu 99.9	Stainless steel 1.430 1	Mild steel 1.033 0
$Na_2S_2O_3.5\,H_2O$	+	+	−	+	+
$Na_2HPO_4.12\,H_2O$	−	−	+	+	+
$CaCl_2.6\,H_2O$	−	−	+	+	+
Loxiol G32		+	+	+	
Lauric acid		+	+	+	

Explanation of symbols :

+ Resistant. — Corrosion rate $\leqslant 0.1$ mm/a.
⊕ Fairly resistant. — Corrosion rate $\leqslant 1.0$ mm/a.
⊖ Not particularly resistant. — Corrosion rate $\leqslant$ 25-30 mm/a.
− Unusable.

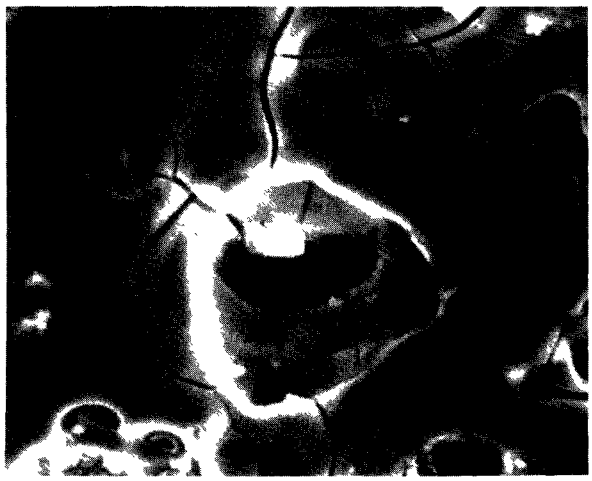

Fig. 21. — SEM photograph of Al 99.5 sample surface showing pitting corrosion after 80 d in $Na_2HPO_4.12\ H_2O$.

of contact time. In general, $AlMg_3$ was found to be more sensitive due its magnesium content. A scanning electron microscopy investigation showed a surface attack after 20 days contact. After 50 days of contact, however, pitting corrosion with trans- and intercrystalline cracks were seen on the aluminum surface, while $AlMg_3$ showed fewer cracks and tended more towards shallow pit formation. These sample surfaces are seen in the scanning electron microscope photographs of figures 21 and 22 for the two samples after 80 d and 105 d in contact with $Na_2HPO_4.12\ H_2O$ respectively.

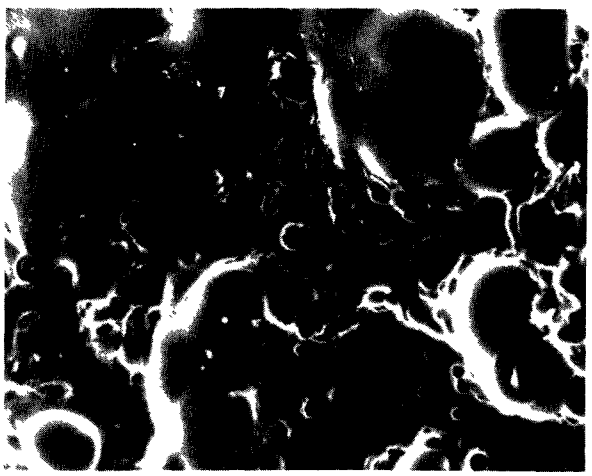

Fig. 22. — SEM photograph of $AlMg_3$ sample surface showing shallow pit formation after 105 d in $Na_2HPO_4.12\ H_2O$.

$CaCl_2.6\ H_2O$ was also found corrosive to aluminum and its alloy $AlMg_3$. Local corrosion in the form of both pitting corrosion and shallow pit formation was also observed in this case.

4.2 HEAT EXCHANGERS. — We have seen earlier in section 4 that a LTES system must possess a heat exchanger for transferring heat from the heat source to the heat storage substance and from the latter to the heat sink. The type of the heat exchanging surface itself plays an important role in the design of LTES systems, as it strongly influences the temperature gradients for charging and discharging of the storage.

4.2.1 *Heat exchanger requirements.* — The LTES heat exchanger must fulfill the following requirements :

1) It should provide for a high effective heat transport rate to allow rapid charging and discharging of the storage. This is a very pressing requirement for latent heat stores as the thermal conductivity of most phase change heat storage materials is extremely low — most of these materials possess insulating properties. A high effective heat rate can be obtained either by embedding a metallic filler of high thermal conductivity within the heat storage medium or by introducing natural or forced convection effects in the storage medium e.g. forced convection through stirring of the medium.

2) It should permit only small temperature gradients for charging and discharging of the storage. This effect may be achieved by providing a substantially large heat transfer surface and small heat transfer paths in the storage medium.

3) The heat exchanger should guarantee a high thermal diffusivity and a high heat diffusivity.

The type of heat exchanger geometries that fulfill these requirements are discussed in the next section.

4.2.2 *Type of heat exchanger geometries.* — LTES heat exchangers fall in 2 categories :

1) passive, i.e. the heat exchanger has no moving parts, and

2) active, i.e. with moving parts.

Passive heat exchangers typically comprise of tubes of small diameter (30-50 mm) or flat pans (20-30 mm deep) within which the phase change material is filled. The tubes can be bundled together as in shell-and-tube type heat exchangers with the heat transfer fluid flowing in the gaps formed between the tubes. Such a configuration is shown in figure 23*a*. Figure 23*b* shows an arrangement wherein the material is sealed into pan-shaped containers. 294 similar pans measuring approximately 520 × 520 × 25 mm and containing 3 000 kg of $Na_2S_2O_3.5\ H_2O$ were stacked together to form a latent heat thermal store for the solar heating system at the University of Delaware [18]. A 10 mm gap was provided between adjacent pans for the circulation of the heat transfer fluid.

Active heat exchangers are those in which means are generally provided to stir the phase change heat

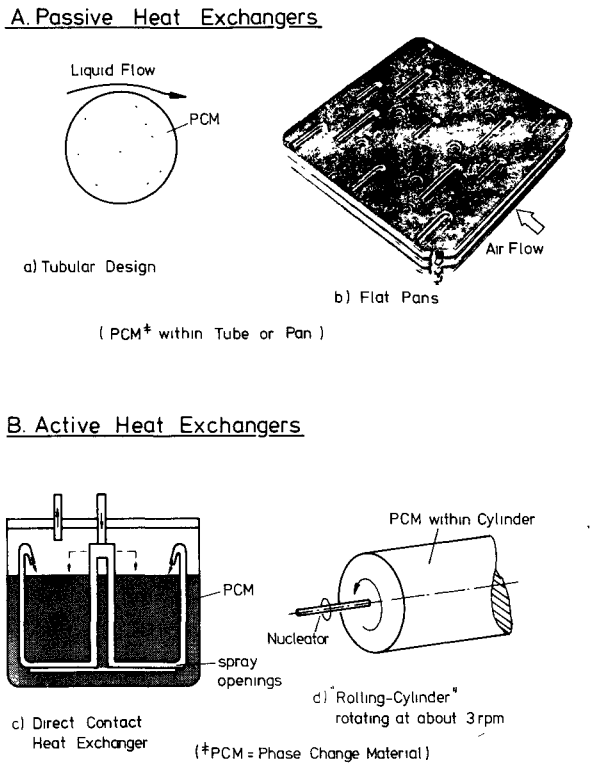

Fig. 23. — Type of heat exchanger geometries considered for LTES systems.

storage material. This is done to improve the heat transfer rate within the storage material, as well as to prevent segregation of phases — a phenomenon typical of inorganic salt hydrates. Two types of active heat exchangers are shown schematically in figures 23*c* and *d*. The heat exchanger in figure 23*c* is a direct contact heat exchanger, so called as the storage material and the heat transfer fluid are brought in direct contact with each other [13]. Hot oil, heated e.g. using a solar collector, is sprayed through fine pores in the solid phase of the phase change material. The large number of oil droplets provide an enhanced heat transfer surface and rapidly transfer their heat to the surrounding salt thereby melting it. When the salt has partially melted, the oil spray creates a turbulence effect in the melt that not only improves the heat transfer rate in the medium, but also prevents segregation of the phases. To remove heat from the storage material, cold oil is sprayed through the liquid phase of the storage material. Thereby heat is removed from the material and salt crystals are formed in the liquid bulk which fall on the container bottom and collect there.

Figure 23*d* is a novel conception of an active heat exchanger — the so called *rolling cylinder* system [7]. The concept which is presently in the laboratory stage comprises of a cylinder filled with sodium-sulphate decahydrate (Glauber salt) that serves as the heat storage material. The cylinder is rotated about its longitudinal axis at about 3 rpm about its axis. The rotation is considered to provide just enough stirring action to keep the temperature of the Glauber's salt uniform and very close to the wall temperature. The researchers involved with the development of this concept believe that under these conditions, the material crystallizes on nuclei in the liquid and not on the cylinder walls. To promote crystal formation, a thin tubular device, called a *nucleator* is inserted through one end of the rotating vessel. The nucleator contains *seed* crystals which act as nucleating agents to initiate the crystallization process when the temperature of the liquid salt drops below its freezing point.

4.2.3 *The finned heat pipe heat exchanger.* — We now wish to discuss in some depth a new type of a passive heat exchanger for LTES systems that is presently under development at the Institut für Kernenergetik und Energiesysteme (IKE) in Stuttgart [2]. The major advantages offered by this heat exchanger are its modular design and flexibility in application in that it can equally well be used with solar collectors utilizing liquid or air as the heat transfer medium.

4.2.3.1 The concept. — Figure 24 shows a schematic of a single heat exchanger module. The module essentially comprises of a container (1) of square cross-section provided with a heat pipe (2) along its longitudinal axis. The container, as well as the heat pipe, are divided into three regions — region A, B and C in figure 1 — by separation walls (5). One of the regions, B, is filled with a heat-of-fusion type storage substance and is called the *Storage Chamber*. The remaining two regions, A and C, are respectively in contact with the fluid, e.g. water or air, flowing through the solar collector and heating load loops, and are termed here as the *Heat Source* and *Heat Sink* regions respectively.

The heat pipe length within the Storage Chamber is provided with closely and equally spaced square fins of large cross-section (3), made from a material of high thermal conductivity, e.g. aluminum. The

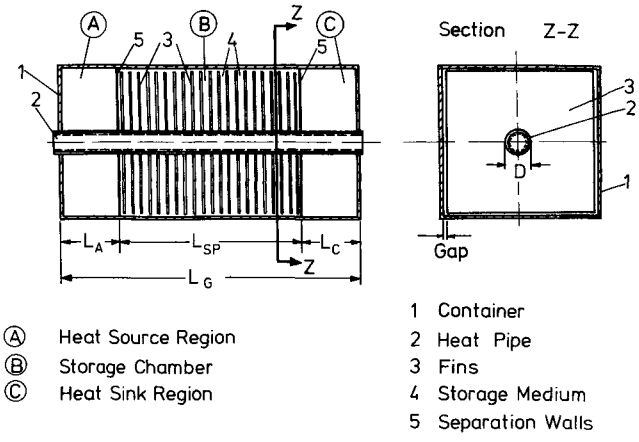

Fig. 24. — Schematic showing the modular finned heat pipe heat exchanger concept [2].

storage medium (4) fills the free volume between the fins. Thus embedded within the storage medium, the fins compensate for its generally poor thermal conductivity and simultaneously ensure small heat flow paths within the LTES system.

The use of the heat pipe offers several advantages and renders flexibility in operation and application. Some of these are :

a) Additional heat exchangers are eliminated. Furthermore, the heat pipe length within the *Heat Source* and *Heat Sink* regions may be suitably finned depending on whether air or liquid is employed as the heat transfer medium in these regions.

b) The heat pipe transports heat under very low temperature gradients so that an almost isothermal heat source in contact with the fins and the thermal storage medium within the Storage Chamber is attained.

c) The heat flux transformation capability of the heat pipe can be utilized to give low heat flux densities within the Storage Chamber for large heat flow rates in the Heat Source/Heat Sink sections.

d) The heat pipe can operate unidirectionally as a diode.

For certain applications where a heat source or heat sink region external to the storage unit are considered advantageous, the finned heat pipe may be replaced by a finned tube, through which the heat transfer fluid, e.g. solar collector liquid, flows. In this case, however, the fluid flowing within the tube experiences a temperature gradient in the direction of flow, so that the isothermality of the heat-carrying tube is lost.

Arrangement of the modules. — Different arrangements of the modules are possible depending on the space available. Two possible arrangements are shown in figure 25. Figure 25*a* shows a so-called *Box-arrangement*, whereby 4 heat pipes are attached to plate fins of square cross-section. Figure 25*b* shows a *Stack arrangement*, which can be particularly useful when only limited space is available. If modules are stacked against a wall, the insulation effect of the wall can additionally be used to the advantage of reducing heat losses from the modules to the surroundings.

4.2.3.2 Performance investigation. — A numerical analysis was undertaken to determine the thermal performance of the Storage Chamber, B, of the module shown in figure 24. The analysis was restricted to the charging of the storage, i.e. melting of the thermal storage substance in the chamber. A module length of 1 m was assumed.

A flowchart summarizing the analysis is presented in figure 26. The thermal performance was assessed in terms of :

a) temperature distribution within the storage medium, fins and heat pipe wall at any time, t;

b) the position of the solid-liquid interface at any time, t;

c) the storage charging time, t_{max}, and

d) the corresponding maximum temperature gradient in the storage chamber, ΔT_{max}, required (at t_{max}) for heat flow into the storage medium as a function of heat flux density.

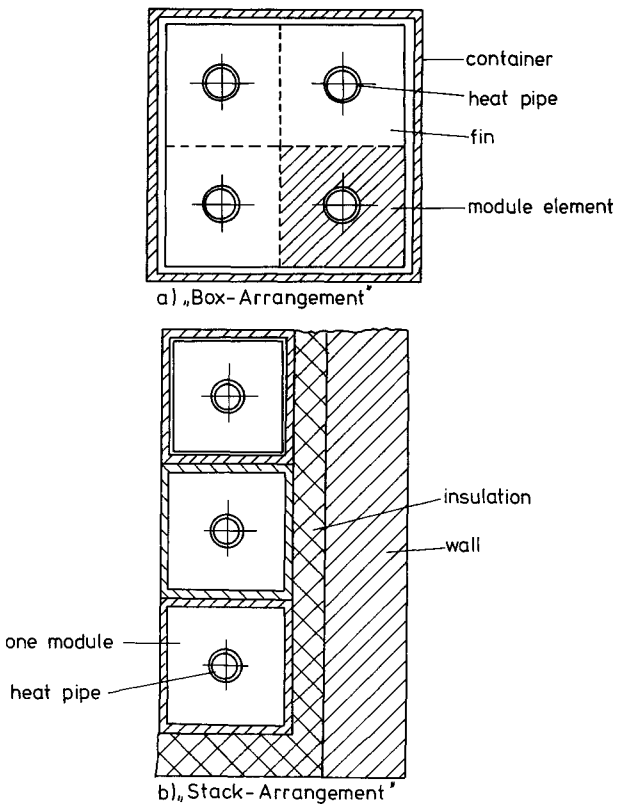

Fig. 25. — Arrangement of the modules.

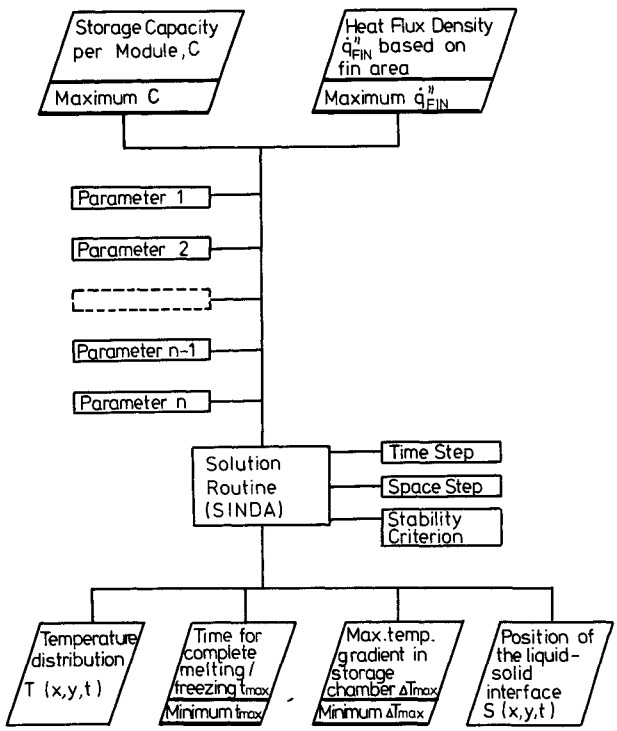

Fig. 26. — Flowchart of the thermal analysis.

The influence of various geometrical parameters such as fin height, fin thickness, fin spacing and void fraction on the thermal performance was investigated. Heat flux densities were assumed to vary between 1 W/cm^2 and 6 W/cm^2 (based on the fin cross-sectional area). The largest module size, and hence the module storage capacity, for acceptable maximum temperature gradients of 5 K and 10 K within the storage chamber was computed.

Two thermal storage substances of particular interest to LTES systems for solar heating applications were selected for the analysis :

(i) Paraffin-white, a paraffin (melting range 48 °C-55 °C) and

(ii) Sodiumthiosulphate-pentahydrate, an inorganic salt (melting range 48 °C-49 °C).

Besides the large difference in their melting range, these two substances differ markedly in their volumetric storage capacities and thermal conductivities. For the same volume, the heat-of-fusion of the salt is approximately 2.5 times that of the paraffin; whereas its thermal conductivity is roughly 3 times as large.

4.2.3.3 Results from the analysis. — A) *Charging time and maximum temperature gradients for heat flow.* — Of particular interest to LTES design are the storage charging time and the maximum temperature gradients required for charging the storage. If the phase change heat storage material does not suffer from any problems with melting and freezing, the charging time becomes a function of the total system storage capacity and the charging rate. The maximum temperature gradient, ΔT_{max}, on the other hand, depends on the heat exchanger geometry — in the present case on the fin dimensions, viz. fin height (DFIN), fin thickness (SR), fin spacing (DR) and the void fraction (SF).

In actual practice, the LTES system heat exchanger for low temperature solar heating applications is constrained to operate within small temperature swings. Consequently the maximum temperature gradient ΔT_{max} is fixed in advance and we proceed to seek the relationship between the fin geometry and the heat flux input rate.

For the computations described here, two values of ΔT_{max} : $\Delta T_{max} = 5$ K and $\Delta T_{max} = 10$ K were selected. For a heat flux input $\dot{q}''_{FIN}$ of 4 W/cm^2 and assuming a void fraction SF of 85 %, the fin dimensions (i.e. fin thickness SR and fin height DFIN) were computed with the aid of the thermal analysis. The results are summed up in table VI for both paraffin-white and sodiumthiosulphate. Also included in the table are the computed values of the module storage capacity per meter length of the module and the relative storage capacity for the different cases considered. For the different cases included in table VI, the variation in module capacity is observed to vary almost six-fold, from a minimum value of 0.31 kWh for paraffin-white ($\Delta T_{max} = 5$ K, SR = 0.9 mm) to a maximum value of 1.91 kWh for thiosulphate ($\Delta T_{max} = 10$ K, SR = 0.3 mm). The example thus demonstrates the importance of the permissible temperature gradients and fin dimensions on the heat storage capability of a single module.

B) *Influence of the melting range.* — The temperature gradients discussed above have been computed using the upper limit of the melting range of the storage substance as the reference temperature. The melting range itself has hence not been explicitly accounted for. In actual practice, the presence of a melting range has an adverse effect on the thermal performance, as its magnitude dictates the temperature swings that a LTES system experiences during heat addition or removal. The total temperature gradient required for storage charging would then be

$$\Delta T_{total} = \Delta T_{max} + \Delta T_{melting\,range} .$$

Figure 27 shows a comparison of ΔT_{max} and ΔT_{total} for a representative module (DFIN = 140 mm, SF = 85 %, SR = 0.5 mm) filled with paraffin and

Table VI. — *Module capacities for selected temperature gradients and fin dimensions.*

Thermal storage substance	Allowable ΔT_{max} (K)	SR (mm)	DFIN (mm)	C (*) (kWh)	Relative storage capacity (**)
Paraffin-white	5	0.3	105	0.41	1.32
		0.9	92	0.31	1.0
	10	0.3	146	0.79	2.55
		0.9	131	0.64	2.06
Sodiumthiosulphate-pentahydrate	5	0.3	107	1.03	3.32
		0.9	96	0.93	3.0
	10	0.3	141	1.91	6.15
		0.9	135	1.75	5.64

(*) C is the module storage capacity per meter length based on the heat-of-fusion of the storage substance only.

(**) The relative storage capacity is defined as the ratio of the storage capacity of any given module to that of a reference module. A paraffin-filled module, for which $\Delta T_{max} = 5$ K and SR = 0.9 mm, is taken as the reference module here. The relative storage capacity of such a module is hence = 1.0.

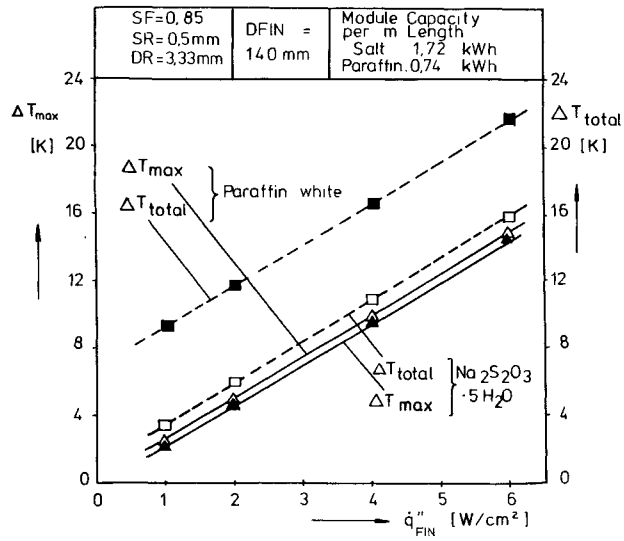

Fig. 27. — Influence of melting range on the maximum temperature gradient.

thiosulphate. Due to the large melting range (7 K) of paraffin-white, rather high total temperature gradients are noticed for complete charging of a module employing paraffin as the storage medium. In other words, such a module would be suitable only if the magnitude of the heat flux density is low, in the range if 1-2 W/cm^2.

4.2.3.4 The test-model. — The heat transfer characteristics of the modular heat exchanger concept were experimentally investigated with the aid of a small 6 liter test-model. Moreover, comparisons were made between experimental data and thermal performance predictions made for the geometry of the test-model using the analysis described above.

Figure 28 shows a photograph of the test-model with the insulation removed. The Storage Chamber consists of a glass cylinder to allow visual observations of the melting and freezing phenomenon within. The finned heat pipe protrudes out from one end of the chamber. This end is alternately heated and cooled, whereby heat flows into the chamber charging the storage medium, or out of it discharging the medium. The relevant geometrical dimensions of the model are given in table VII.

Paraffin-white was used as the storage substance during the tests. The storage capacity of the storage chamber was estimated to be 220 Wh.

The model was well-instrumented with 41 nickel-chrome-nickel thermocouples to provide information on the temperature distribution along the heat pipe, the fin surface and within the storage medium. Following preliminary testing, the temporal variation of the output of 30 selected thermocouples was monitored using a Philips 24-point recorder and a Linseis 6-channel stripchart recorder.

Table VII. — *Dimensions of the testmodel.*

Storage chamber :	length = 800 mm, inner diameter = 104 mm.
Heat pipe :	length = 1 200 mm, outer diameter = 20 mm.
Fins :	outer diameter = 100 mm, thickness = 0.6 mm, mean spacing between adjacent fins = 6 mm.
Storage chamber volume :	6 liter.

Heat transport capacity of the heat pipe : 1 000 W at 50 °C.

4.2.3.4.1 *Experimental results.* — Heating and cooling curves were obtained with the test model for different heat input/output rates. An evaluation of these curves showed that paraffin-white possessed large unidentical melting and freezing ranges. The melting range was spread over 9 K, from 47 °C to 56 °C, which is somewhat larger than the range assumed for the analysis.

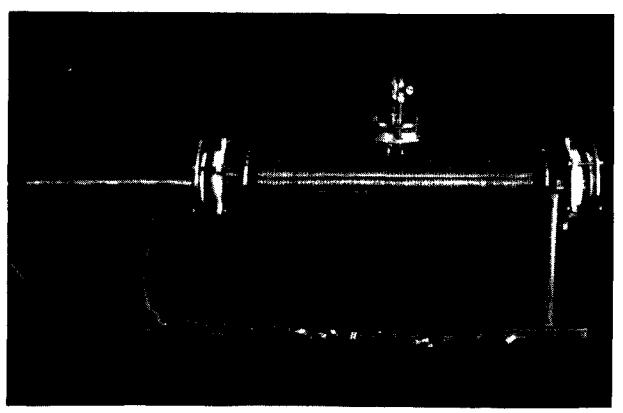

Fig. 28. — The testmodel.

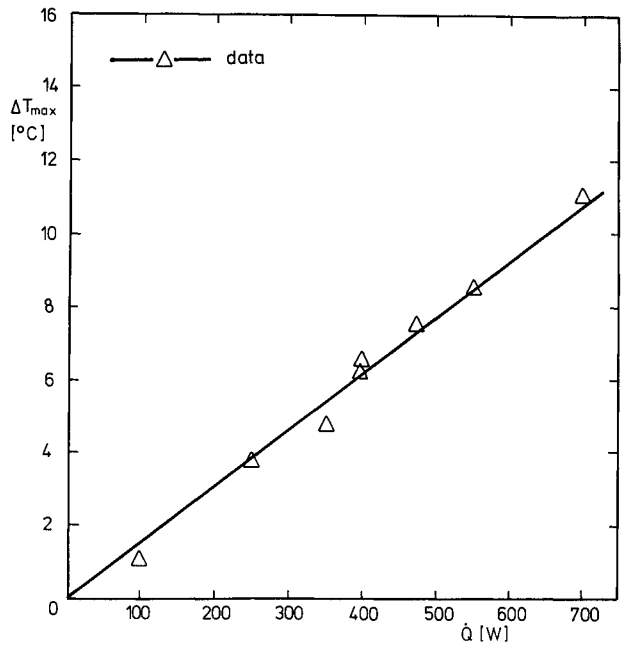

Fig. 29. — Maximum temperature gradients as a function of heat input rate.

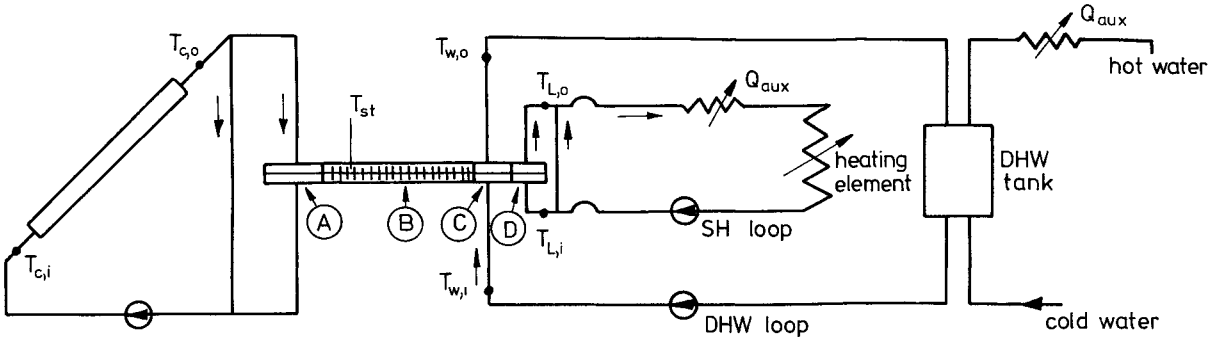

Ⓐ Heat source region
Ⓑ Storage chamber
Ⓒ Heat sink region for hot water
Ⓓ Heat sink region for space heating

SH loop-Space heating loop
DHWloop-Domestic hot water loop

$T_{c,i}$, $T_{c,o}$ = Inlet and outlet temperature of collector fluid
T_{st} = Temperature of the heat storage material
$T_{w,i}$, $T_{w,o}$ = Inlet and outlet temperature of hot water
$T_{L,i}$, $T_{L,o}$ = Inlet and outlet temperature of the fluid flowing through the heating element
Q_{aux} = Auxiliary energy

Fig. 30. — Integration of the finned heat pipe exchanger in a solar heating system.

In addition, the maximum temperature gradient, ΔT_{max}, in the test-model was experimentally determined as a function of the heat input rate $\dot{Q}$. The heat input range was varied between 100 W and 700 W, corresponding to a heat flux density range ($\dot{q}''_{FIN}$) of 1.3 and 9.1 W/cm^2 based on the fin area, or a heat flux density range ($\dot{q}''_{HP}$) of 0.2-1.4 W/cm^2 based on the heat pipe surface area.

Figure 29 shows the variation of ΔT_{max} with the heat input rate. A linear relationship, indicative of conductive heat transfer in the medium, is observed. It is interesting to note that in spite of the very poor thermal conductivity of paraffin (k = 0.175 W/mK), the temperature gradients are rather small and lie around 8 K for a heat input rate of 500 W (corresponding $\dot{q}''_{FIN}$ = 6.5 W/cm^2, $\dot{q}''_{HP}$ = 1.0 W/cm^2).

4.2.3.5 Integration of the LTES in a solar space heating and hot water production system. — Figure 30 shows a system schematic of a possible solar heating system using the finned heat pipe LTES concept discussed above. The heat pipe is divided in 4 regions : region A is in contact with the solar collector fluid, region B is the storage chamber, region C is connected to the hot water loop and region D to the space heating loop. The respective inlet and outlet temperatures are marked on the diagram.

Heat entering region A is transported axially along the heat pipe to the thermal store B, or to the load loops via the heat exchangers in the regions C and D. If a simultaneous supply of solar energy and load demand exists, the storage is more-or-less bypassed, as the heat transfer in regions C and D is far better than in region B. On the other hand, when little or no load exists in regions C and D the thermal store in region B is charged.

When no solar energy is available, the collector loop in region A is shut off. The storage then supplies its heat to the regions C and D with the help of the heat pipe and, in turn, gets discharged. In case more energy is needed than the storage can deliver, the auxiliary heaters are automatically turned on.

5. **Cost of heat storage.** — Cost calculations for factory-produced thermal storage subsystems are presently available only for hot water storage. Cost estimations for latent heat stores are essentially based on function models of laboratory devices and are hence rather unreliable.

Figure 31 shows the specific cost of hot water storage subsystems as a function of storage volume [3]. The diagram includes actual cost of small capacity stores marketed in Europe and projected costs for large-scale storage. There is a large spread in cost, the specific cost of the storage varying by a factor 5-25 for the same volume as seen in table VIII.

The large cost range reflects the uncertainty that exists even today for the hot water stores.

Figure 31 reveals that a definite cost degression is present as the storage capacity experiences a transition from small-scale to large-scale. Thus, medium-sized storage subsystems, such as those for the seasonal heating of houses in a small community, are particularly attractive from a cost viewpoint.

Table VIII. — *Cost of hot water storage subsystem* [3].

Storage capacity [m^3]	Specific cost Lower limit [DM/l]	Specific cost Upper limit [DM/l]	Cost of storage subsystem Lower limit [DM]	Cost of storage subsystem Upper limit [DM]
—	—	—	—	—
0.5	3.–	15.–	1 500.–	7 500.–
5.0	0.50	6.–	2 500.–	30 000.–
50.0	0.10	1.–	5 000.–	50 000.–
10^4	0.028	0.50	28×10^4	5×10^6
10^7	0.01	0.25	100×10^6	2.5×10^9

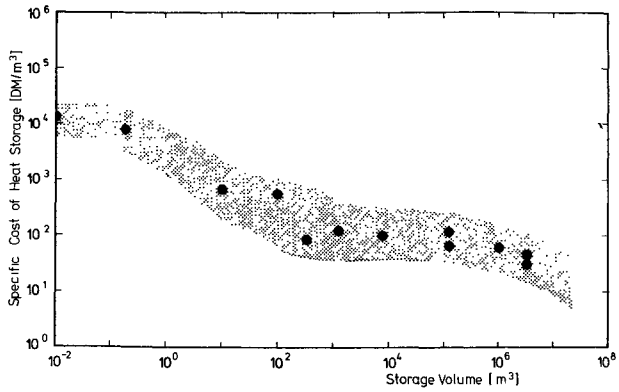

Fig. 31. — Specific cost of heat storage [3].

6. **Concluding remarks.** — Sensible heat storage and latent heat storage are the two major techniques for thermal energy storage considered today for low temperature uses of solar energy, such as space heating and hot water production. Sensible heat storage, wherein energy is stored in water or rocks, is presently in an advanced stage of development and is readily available as a component of solar heating systems. Latent heat storage, on the other hand, is a developing technology that has been found very promising in recent times due to the several operational advantages it offers, viz. smaller temperature swings, lower required solar collector temperature, and smaller size and lower weight per unit of storage capacity.

Hot water storage subsystems for solar heating systems must be designed to ensure stratification, whereby the net energy gain from the sun can be increased by 10-15 %. Furthermore, practical requirements for storage installation, integration with the residential structure, storage life, cost, etc. must be given due consideration.

In the development of latent heat storage systems, research in underway in two directions : investigation of phase change heat storage materials and heat exchangers. The melting/freezing characteristics of the heat storage materials, their ability to undergo thermal cycling and their compatibility with construction materials is important for the life of the LTES systems. Heat exchangers must ensure that extreme conditions of charging and discharging are met, whereas the necessary temperature gradients for charging and discharging are small. A number of problems, however still remain to be tackled before technically and economically favourable LTES systems can be made available for widespead use.

Acknowledgment. — A part of the work reported here was carried out under Grant No. ET 4060 A of the German Ministry for Research and Technology (BMFT).

References

[1] ABHAT, A., ABOUL-ENEIN, S. and NEUER, G., « Latentwärmespeicher zur Verwendung in Solar-Energiesystemen für Wohngebäude », VDI-Berichte Nr. 288 (1977).

[2] ABHAT, A., « Performance Studies of a Finned Heat Pipe Latent Heat Thermal Energy Storage System », Proceedings of the 77 International Solar Energy Congress, New Delhi (1978).

[3] BELL, C. R., JÄGER, F. and KORZEN, W., « Systemstudie über die Möglichkeiten einer stärkeren Nutzung der Sonnenenergie in der Bundesrepublik Deutschland », Sonnenenergie II, Umschau Verlag, Frankfurt, 1977.

[4] BISWAS, D. R., « Thermal Energy Storage using Sodium Sulphate Decahydrate and Water », *Sol. Energy*, **19** (1977) 99-100.

[5] DAVIS, E. S. and BARTERA, R., « Stratification in Solar Water Heater Storage Tanks », Proceedings, Workshop on Solar Energy Storage Subsystems for the Heating and Cooling of Buildings, Charlottesville, Virginia, April 1975.

[6] Dechema Werkstoff Tabellen, Chemische Beständigkeit, Dechema, Frankfurt.

[7] General Electric's « Rolling Cylinder » Heat Storage Device, Mechanical Engineering, March 1978.

[8] GREEN, H. S., *The Molecular Theory of Fluids* (Interscience Publishers, New York) 1952.

[9] HAASEN, P., *Physik. Metal.* (Springer-Verlag, Heidelberg) 1974.

[10] HEINE, D. and ABHAT, A., « Investigation of Physical and Chemical Properties of Phase Change Materials for Space Heating/Cooling Applications », Proceedings of the 77 International Solar Energy Congress, New Delhi (1978).

[11] HEINE, D., « Korrosionsuntersuchungen an Materialien für den Einsatz in Latentwärmespeichern », VDI-Berichte Nr. 288 (1977).

[12] LANE, G. A. and GLEW, D. N., « Heat-of-Fusion Systems for Solar Energy Storage », Proceedings of the Workshop on Solar Energy Storage Subsystems, Charlottensville, Virginia (1975).

[13] LINDNER, F., « Physikalische, chemische und technologische Grundlagen der Latentwärmespeicherung », in Grundlagen der Solartechnik, Proceedings of the Meeting of the German Solar Energy Society, Stuttgart-Fellbach (1976).

[14] LORSCH, H. G., KAUFFMAN, K. W. and DENTON, J. C., « Thermal Energy Storage for Solar Heating and Off-Peak Airconditioning », *Energy Conversion*, **15** (1975) 1-8.

[15] PICKERING, E. E., « Residential Hot Water Solar Energy Storage Subsystems », Report NSF RA-N-75-095, Stanford Research Institute, Menlo Park, California, January 1976.

[16] SHARP, M. K. and LOEHRKE, R. I., « Stratified Versus Well-Mixed Sensible Heat Storage in a Solar Space Heating Application », Paper No. 78-HT-49, Presented at the AIAA-ASME Thermophysics and Heat Transfer Conference Palo Alto, California, May 1978.

[17] STRICKLAND-CONSTABLE, R. F., *Kinetics and Mechanisms of Crystallization* (Academic Press, London) 1968.

[18] TELKES, M., *Storage of Solar Heating/Cooling* (ASHRAE Transactions), vol. **80** (1974).

[19] TELKES, M., « Solar Energy Storage », ASHRAE Journal (1974).

[20] TELKES, M., « Thermal Storage of Solar Heating and Cooling » Proceedings of the Workshop on Solar Energy Storage Subsystems, Charlottensville, Virginia (1975).

[21] ZIEF, M. and WILCOX, W. R., *Fractional Solidification* (Marcel Dekker, Inc., New York), vol. **1**, 1967.

Appendix. — *Comparison between water storage, storage in rock beds and latent heat storage in phase change materials.*

Figure A1 shows a schematic of the three types of thermal stores discussed in the text. Typical values of some relevant properties of heat storage materials used in these thermal stores are given below in table A. 1 for comparison. The last column in table A. 1 gives the relative volume occupied by each of the storage media for a heat storage capacity of 10^6 kJ and a temperature rise of 15 K during heat storage.

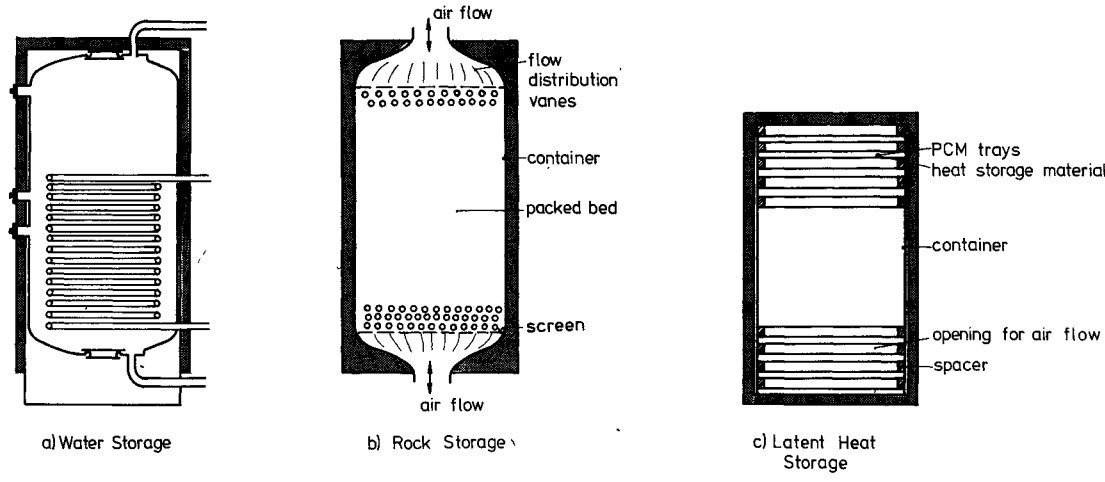

Fig. A1. — Schematics of water, rock and latent heat stores.

Table A1. — *Comparison of various heat storage media* (stored energy = 10^6 kJ = 300 kWh ; ΔT = 15 K).

	Heat storage material			
	Sensible heat storage		Latent heat storage	
Property	Rock	Water	Organic phase change materials	Inorganic phase change materials
Latent heat of fusion (kJ/kg)	— (*)	— (*)	190	230
Specific heat (kJ/kg)	1.0	4.2	2.0	2.0
Density (kg/m^3)	2 240	1 000	800	1 600
Storage mass for storing 10^6 kJ (kg)	67 000	16 000	5 300	4 350
Relative mass (**)	15	4	1.25	1.0
Storage volume for storing 10^6 kJ (m^3)	30	16	6.6	2.7
Relative volume (**)	11	6	2.5	1.0

(*) Latent heat of fusion is not of interest for sensible heat storage.
(**) Relative mass and volume are based on latent heat storage in inorganic phase change materials.